1	Plant leaf wax biomarkers capture gradients in hydrogen isotopes of precipitation from the
2	Andes and Amazon
3	Sarah J. Feakins* <sup>a</sup> ; Lisa Patrick Bentley <sup>b</sup> ; Norma Salinas <sup>b,1</sup> ; Alexander Shenkin <sup>b</sup> ; Benjamin
4	Blonder <sup>b</sup> ; Gregory R. Goldsmith <sup>b</sup> ; Camilo Ponton <sup>a</sup> ; Lindsay J. Arvin <sup>a</sup> ; Mong Sin Wu <sup>a</sup> ; Tom
5	Peters <sup>s</sup> ; A. Joshua West <sup>a</sup> ; Roberta E. Martin <sup>c</sup> ; Brian, J. Enquist <sup>d</sup> ; Gregory, P. Asner <sup>c</sup> ; Yadvinder
6	Malhi <sup>b</sup>
7	<sup>a</sup> Department of Earth Sciences, University of Southern California, Los Angeles, CA 90089,
8	USA.
9	<sup>b</sup> Environmental Change Institute, School of Geography and the Environment, University of
10	Oxford, Oxford, OX1 3QY, UK.
11	<sup>c</sup> Department of Global Ecology, Carnegie Institution for Science, Stanford, CA 94305, USA.
12	<sup>d</sup> Department of Ecology and Evolutionary Biology, University of Arizona, AZ 85721, USA.
13	
14	
15	
16	
17	
18	
19	
20	*Corresponding author: Sarah J. Feakins, email: <u>feakins@usc.edu</u> , phone: 213 740 7168
21 22	<sup>1</sup> Permanent address: Seccion Química, Pontificia Universidad Católica del Peru, Peru.
23	Author Contribution Statement
24 25 26 27 28 29	S.J.F planned and designed the leaf wax and plant water study; Y.M. conceived the field campaign; Y.M. B.J.E., G.P.A., L.P.B., N.S., G.R.G. and A.S., designed the CHAMBASA field campaign; A.J.W and S.J.F. designed the stream and precipitation sampling. S.J.F. performed plant water extractions and leaf wax isotopic analyses; M.S.W., T.P., L.J.A., analyzed leaf wax concentrations; C.P. sampled streams and analyzed stream water and precipitation. L.P.B., N.S., A.S., B.B., G.R.G., conducted CHAMBASA fieldwork. R.E.M. led taxonomy. S.J.F., L.P.B., A.S., B.B., C.P., M.S.W., T.P., analyzed aspects of data and S.J.F. wrote the manuscript.
	, , , ,,,, or and and court wrote me management

#### Abstract

32

33

34

35

36

37

38

39

40

41

42

43

44

45

46

47

48

49

50

51

52

Plant leaf waxes have been found to record the hydrogen isotopic composition of precipitation and are thus used to reconstruct past climate. To assess how faithfully they record hydrological signals, we characterize leaf wax hydrogen isotopic compositions in forest canopy trees across a highly biodiverse, 3 km elevation range on the eastern flank of the Andes. We sampled the dominant tree species and assessed their relative abundance in the tree community. For each tree we collected xylem and leaf samples for analysis of plant water and plant leaf wax hydrogen isotopic compositions. In total, 176 individuals were sampled across 32 species and 5 forest plots that span the gradient. We find both xylem water and leaf wax  $\delta D$  values of individuals correlate  $(R^2 = 0.8 \text{ and } R^2 = 0.3 \text{ respectively})$  with the isotopic composition of precipitation (with an elevation gradient of -21% km<sup>-1</sup>). Minimal leaf water enrichment means that leaf waxes are straightforward recorders of the isotopic composition of precipitation in wet climates. For these tropical forests we find the average fractionation between source water and leaf wax for C<sub>29</sub> nalkanes,  $-129 \pm 2\%$  (s.e.m., n = 136), to be indistinguishable from that of temperate moist forests. For  $C_{28}$  *n*-alkanoic acids the average fractionation is  $-121 \pm 3\%$  (s.e.m., n = 102). Sampling guided by community assembly within forest plots shows that integrated plant leaf wax hydrogen isotopic compositions faithfully record the gradient of isotopes in precipitation with elevation ( $R^2 = 0.97$  for *n*-alkanes and 0.60 for *n*-alkanoic acids). This calibration study supports the use of leaf waxes as recorders of the isotopic composition of precipitation in lowland tropical rainforest, tropical montane cloud forests and their sedimentary archives.

**Keywords:** Andes; Amazon; biomarker; ecohydrology; hydrogen isotopes; leaf wax.

#### 1. INTRODUCTION

54

55 Tropical forests are some of the most productive and diverse ecosystems on the planet. They are significantly threatened by deforestation (e.g., Malhi et al., 2014b) and projected climate change 56 (Cox et al., 2004; Oyama and Nobre, 2003) including the possibility of changes in hydrological 57 cycling (Zelazowski et al., 2011). If we want to better monitor and track how hydroclimate 58 affects tropical forests, then the hydrogen and oxygen isotopic composition of water can provide 59 us with valuable insights, including into seasonality and precipitation amounts (Lee et al., 2009). 60 At the scale of the Amazon basin, the isotopic composition of precipitation is dependent upon 61 atmospheric circulation and rainout, as well as vapor recharge with transpiration from the forest 62 (Salati et al., 1979). Isotopes have the potential to be powerful tracers of change in the 63 ecosystem-atmosphere water cycle at the continental scale, particularly when sampling schemes 64 capture precipitation isotope gradients (Winnick et al., 2014). Uptake of water by plants leads to 65 66 the isotopic composition of precipitation being encoded in the hydrogen isotopic composition of plant waxes, including those on tree leaves (Sachse et al., 2012). These waxes survive long 67 beyond the life of the plant to become molecular fossils or 'biomarkers' in geological archives 68 and are commonly used to reconstruct past hydrological conditions (Feakins et al., 2012; 69 Schefuss et al., 2005; Tierney et al., 2013). 70 Fundamental to this approach is the observation that the isotopic composition of source water 71  $(\partial D_w)$ , usually precipitation, is translated into that of leaf wax  $(\partial D_{wax})$  after a large 'apparent' 72 fractionation ( $\varepsilon_{app}$ ) the net effect of multiple fractionation steps (Sachse et al., 2012). The 73 biosynthetic fractionation ( $\varepsilon_{bio}$ ) associated with the synthesis of wax, comprises the major isotope 74 effect at c. -160% (Sessions et al., 1999). While commonly assumed to be relatively invariant, 75

 $\varepsilon_{\rm bio}$  does vary with the use of stored versus primary photosynthate such as across the growing season (Newberry et al., 2015; Sessions, 2006). While  $\varepsilon_{bio}$  may also vary between organisms and ecosystems (Kahmen et al., 2013b), tropical forests are unknown in this regard. A secondary effect on isotope fractionation is the net enrichment between precipitation and leaf water, whether in soils (evaporation) or in the leaf (associated with processes of transpiration and atmospheric vapor exchange; expressed as the enrichment of bulk leaf water over xylem water  $\varepsilon_{LW/XW}$ ) (Feakins and Sessions, 2010; Kahmen et al., 2013b; Kahmen et al., 2013a; Smith and Freeman, 2006). As both processes are modulated by climate (including relative humidity and temperature) and ecology (for example rooting strategies and monocot versus dicot leaves), this motivates calibration in different climatic conditions and ecosystems. Calibration studies of leaf wax hydrogen isotope systematics in living plants have included temperate zones (Hou et al., 2007; Sachse et al., 2006; Tipple and Pagani, 2013), arid zones (Feakins and Sessions, 2010; Kahmen et al., 2013b; Smith and Freeman, 2006) and high latitudes (Shanahan et al., 2013; Wilkie et al., 2013), but not yet tropical forests. Leaf water model predictions suggest that  $\varepsilon_{LW/XW}$  will be minimal in wet climates <20% (Kahmen et al., 2013b; West et al., 2008), a prediction that we directly test in this study with combined plant water and wax measurements. A critical next step in understanding plant wax hydrogen isotope biogeochemistry toward global calibration of the proxy is to establish how the hydrogen isotopic composition of source water  $(\delta D_w)$  translates into that of leaf wax  $(\delta D_{wax})$  in tropical forests, including lowland rainforests and tropical montane broadleaf forests. Such studies of tropical hydrogen isotope biogeochemistry will inform tropical paleoenvironmental interpretations.

## 1.1. Tropical rainforests

76

77

78

79

80

81

82

83

84

85

86

87

88

89

90

91

92

93

94

95

96

The forests of the western Amazon are notably some of the most diverse ecosystems in the world (Kreft and Jetz, 2007) which includes not only high species diversity (Ter Steege et al., 2010), but also high diversity in plant functions (Silman, 2014). The absence of prior studies of hydrogen isotopes in living plants in tropical lowland rainforest ecosystems leaves many open questions, and not least of these is the overriding question about how well these proxy recorders will work in the context of tropical climates and high biodiversity. Specific questions include whether there are interspecies variations in plant water systematics (such as might be associated with the physiology of the roots and leaves) that may impact plant water isotopic compositions (Gao et al., 2015; Krull et al., 2006), or whether these physiological and plant water regulation concerns are mitigated in high humidity, tropical climates? In the context of taxonomic diversity, are there variations in biosynthetic fractionations that might be related to plant functional differences (including differing metabolic pathways, use of stored carbohydrates and seasonality of growth strategies)? To begin to collect data to address these and other questions, we set out to collect a large ecosystem-scale survey of plant water and leaf wax isotopic compositions for tree species from forest plots in a transect that extends through western Amazonian, lowland rainforest and up through Andean tropical montane cloud forests.

## 1.2. Tropical montane cloud forests

98

99

100

101

102

103

104

105

106

107

108

109

110

111

112

113

114

115

116

117

118

119

Cloud forests are those forests that are frequently or persistently immersed in ground level cloud (i.e. fog) and include lowland coastal forests such as the Redwoods of California (Dawson, 1998), but cloud forests are most widely distributed in tropical mountains with over 560 confirmed tropical montane cloud forest regions (Bruijnzeel et al., 2011). Estimates of the global areal extent of tropical montane cloud forests range from 215 000 km², based on typical

elevation distributions (800 to 3500 m elevation), to 2 210 000 km<sup>2</sup>, based on satellite estimates of cloud extent (Bruijnzeel et al., 2011). In the Andes, cloud forest occurs between ~1500–3500 m asl (Bruijnzeel et al., 2011). Although less diverse than the lowland rainforests below, tropical montane cloud forests (TMCF) are recognized as biodiversity 'hotspots', i.e. regions of notable biodiversity that are under threat of habitat loss (Myers et al., 2000), whether due to deforestation or changing cloud frequencies associated with temperature rise. This vulnerability is also of concern downstream, given the role of these forest ecosystems in regulating catchment hydrology (Viviroli et al., 2007). In terms of isotope biogeochemistry, it has been suggested that cloud forests may have unique isotope systematics based on an evolved capacity for foliar water uptake (Goldsmith et al., 2013). We expect to see isotopic signatures associated with the uptake of fog waters that would suppress the D-enrichment of leaf waters during transpiration that has been reported in low relative humidity environments (Feakins and Sessions, 2010). Plant water and wax hydrogen isotope systematics in high precipitation (2–5 m a<sup>-1</sup>) and sometimes cloudimmersed forests (above 1500 m) are assessed as part of this survey of tropical forests across a 3 km elevation range.

#### 1.3. Elevation gradients

120

121

122

123

124

125

126

127

128

129

130

131

132

133

134

135

136

137

138

139

140

141

Elevation transect studies uniquely capture a wide range of environmental conditions within a relatively small spatial scale (Becker et al., 2007; Malhi et al., 2010). The 'altitude effect', i.e., change in the isotopic composition of precipitation with elevation (Gonfiantini et al., 2001), provides the opportunity to capture a large range of isotopic values. Like many other spatial transects, elevation profiles sample shifts not only in the isotopic composition of precipitation but also in other environmental parameters including mean annual temperature, the amount and

seasonality of precipitation, relative humidity, cloud immersion frequency, ultraviolet radiation and atmospheric pressure and partial pressures. These parameters contribute to vegetation transitions and each may affect isotopic compositions. Other calibration studies comparing the D of precipitation and plant leaf wax biomarkers have included latitudinal, altitudinal and continental transects of modern plants (Feakins and Sessions, 2010; Kahmen et al., 2013b; Sachse et al., 2006; Smith and Freeman, 2006; Tipple and Pagani, 2013), soils (Bai et al., 2015; Ernst et al., 2013; Jia et al., 2008; Peterse et al., 2009), lake sediments (Hou et al., 2008; Polissar and Freeman, 2010; Sachse et al., 2004), and river sediments (Galy et al., 2011; Ponton et al., 2014). Prior studies across elevation gradients have suggested that plant leaf wax hydrogen isotopic compositions in soils or rivers do capture elevation gradients in the isotopic composition of precipitation (Bai et al., 2015; Ernst et al., 2013; Galy et al., 2011; Jia et al., 2008; Luo et al., 2011; Ponton et al., 2014), and this leaf wax method has been applied to ancient sediments to reconstruct precipitation isotopes for paleoaltimetry (Hren et al., 2010; Polissar et al., 2009). While the expected altitude effect has been shown in 6 species (2 conifers, 2 deciduous trees, 2 shrubs) growing between 2900 and 4200 m on the Tibetan Plateau at 29 °N (Bai et al., 2011), the altitudinal isotope effect has not yet been broadly established in living vegetation. Most prior plant-based calibration efforts have employed small numbers of dominant species (Sachse et al., 2006; Tipple and Pagani, 2013). Such studies have demonstrated the expression of the leaf wax proxy in individual species and have revealed differences between species (Kahmen et al., 2013b). In the tropics, in montane regions and across many strong climatic gradients, plant community turnover, i.e. beta diversity (Condit et al., 2002), presents situations where it is impossible to follow a single species over the distances required to track gradients in the isotopic

142

143

144

145

146

147

148

149

150

151

152

153

154

155

156

157

158

159

160

161

162

composition of precipitation. We suggest that tropical species-richness (alpha diversity) and turnover (beta diversity) should not be seen as obstacle to effective calibration, but rather we embrace the complexity of these ecosystems as directly of interest, and we aim to collect large, community-representative samples.

## 1.4 Andes-Amazon tropical forest hydrogen isotope calibration

164

165

166

167

168

169

170

171

172

173

174

175

176

177

178

179

180

181

182

183

184

In order to advance the use of the plant wax hydrogen isotope proxy for reconstruction of past variations in tropical climates, we conduct a large-scale calibration study in one of the major tropical forests of the world today, including the western Amazonian lowland rainforests and the upland forests of the Peruvian Andes. This transect provides a large precipitation isotopic range (>60‰) for effective calibration. We sample plant leaf waxes, leaf water, stem water and precipitation to directly determine hydrogen isotopic fractionations, using a paired ecohydrological and organic geochemical approach previously used to characterize hydrogen isotope systematics in dry, subtropical southern California (Feakins and Sessions, 2010). We incorporate dual hydrogen and oxygen isotope analysis of environmental waters and plant waters to resolve water sources and to constrain whether plants are accessing water on the local meteoric water line (LMWL); to test for the use of waters that are evaporatively-enriched (deemed unlikely in this very wet climate) and to test for the (likely) use of cloud water sources in TMCF ecosystems (Goldsmith et al., 2013), as can be observed from D-excess above the LMWL (Clark et al., 2014). In order to characterize highly biodiverse tropical ecosystems, we sample a large number of

individuals and account for community-representation in order to determine the hydrogen

isotopic biogeochemical fractionations and compositions relevant at the ecosystem- and landscape-scale. Our approach weights for the waxiness of leaves and the relative abundance of tree species in order to link between leaf-level calibration sampling and landscape-level sedimentary application. We hypothesize that leaf wax traits will on average record the hydrogen isotopic composition of precipitation. At the individual level we expect isotopic variability in plant water sourcing and biological fractionations based on plant physiological and biochemical differences.

By sampling across species, forest plots and elevation, we seek data to support the use of leaf wax biomarkers as a paleohydrological proxy in tropical forests. Specifically, we seek to determine whether ecosystem-scale sampling of living plants' leaf wax biomarkers record local meteoric water isotopic composition in tropical forest ecosystems. We conclude with recommendations for further calibration and application of these plant leaf wax biomarker hydrogen isotopic approaches to reconstruct paleoenvironments.

#### 2. MATERIALS AND METHODS

2.1. Study location

199

200

220

This study included 5 plots (Table 1) that belong to a group of permanent 1-ha plots operated by 201 202 the Andes Biodiversity Ecosystems Research Group (ABERG, 203 http://www.andesconservation.org) and that are part of the ForestPlots (https://www.forestplots.net/) and Global Ecosystems Monitoring (GEM; 204 http://gem.tropicalforests.ox.ac.uk/projects/aberg) networks. 205 Three montane plots are located in the Kosñipata Valley in the province of Paucartambo, 206 department of Cusco, Peru, and two lowland plots are located in Tambopata in the department of 207 Madre de Dios, Peru (Malhi et al. 2010). All plots are located in areas that have relatively 208 209 homogeneous soil substrates and stand structure and minimal evidence of human disturbance (Girardin et al., 2014b). The lowland plots were established in the early 1980s, and the montane 210 ones between 2003 and 2013, with all stems >10 cm diameter at breast height tagged and 211 212 identified to species-level. Plots have been annually measured for carbon allocation and cycling following the standard GEM Network protocol (Marthews et al. 2014). As such, net primary 213 productivity estimates (Girardin et al., 2010) and comprehensive descriptions of the carbon cycle 214 exist for all of these plots (Girardin et al., 2014a; Huacara Huasco et al., 2014; Malhi et al., 215 216 2014a; Malhi et al., 2015). The field-plots are located across the Andes-Amazon elevation gradient, including upper TMCF, 217 lower TMCF and lowland rainforest (Table 1; Fig. 1). Mean annual temperature (MAT) declines 218 with increasing elevation from 24.4 to 13.1°C. Mean annual precipitation (MAP) increases from 219 1900 mm yr<sup>-1</sup> in the lowlands to 5302 mm yr<sup>-1</sup> in the lower TMCF close to the cloud base and

then declines again to 1560 mm yr<sup>-1</sup> in the upper TMCF (Girardin et al., 2014a; Huacara Huasco et al., 2014; Malhi et al., 2014a; Rapp and Silman, 2012). There is a distinct seasonality in the amount of precipitation with 200-800 mm month<sup>-1</sup> precipitation occurring during the November-March wet season and ~100 mm month<sup>-1</sup> in the June-August dry season (Girardin et al., 2014a; Rapp and Silman, 2012). In the montane forest plots, cloud immersion is most common in the dry season (April-September).

## 2.2. Meteoric water sampling

Integrated measures of precipitation isotopes were collected every ~2 weeks for one year using samplers containing mineral oil. The stable H and O isotopic composition of precipitation was measured by laser spectroscopy.  $\delta D$  and  $\delta^{18}O$  values were measured simultaneously on 8 replicate injections of 0.7 uL water using a Los Gatos Research DLT-1000 liquid water isotope analyzer at the California Institute of Technology. Hydrogen and oxygen isotope ratios (as D:H and  $^{18}O$ : $^{16}O$  respectively) are expressed in delta notation as 'per mil' or parts per thousand (‰) relative to the Vienna Standard Mean Ocean Water (VSMOW)-Standard Light Antarctic Precipitation (SLAP) isotopic scale with accuracy determined to better than 0.2‰ and 0.1‰, respectively. Replicate measurements yielded a mean precision ( $\sigma$ ) of 0.5‰ for  $\partial D$  and 0.2‰ for  $\partial A^{18}O$  (n=43) and were calibrated using 3 working standards (Maui Water,  $\partial D=-10.6\%$ ,  $\partial A^{18}O=-3.3\%$ , Caltech internal standard,  $\partial D=-73.4\%$ ,  $\partial A^{18}O=-9.7\%$ ; and LGR Water # 2,  $\partial D=-117.0\%$   $\partial A^{18}O=-15.5\%$ ).

gradient, we sampled small upland streams and lowland tributaries, each of which were selected

for their restricted elevation range catchments. In this way these samples represent the local water composition at the sampling site. We do not consider river water isotopic composition from the main stem or large tributaries which transport water from higher elevations to the sampling location. Our stream water samples were measured with the same methods described above for precipitation samples and the results were previously reported for hydrogen isotopes (Ponton et al., 2014). Here we re-evaluate these data for their dual isotopic composition and compare to our biweekly precipitation isotope collections described above, as well as prior collections of precipitation and cloud water (Clark et al., 2014; Horwath, 2011) in order to understand meteoric waters across the transect.

## 2.3. Leaf sampling

From April – November 2013 (dry season), we measured plant traits as part of the CHAMBASA (CHallenging Attempt to Measure Biotic Attributes along the Slopes of the Andes) project.

Based on the most recently available census and diameter data, a sampling protocol was adopted wherein species were sampled that maximally contributed to plot basal area (a proxy for plot biomass or crown area). At each site at least five species were sampled for plant water and wax analysis. Within each species, three individual trees were chosen for sampling. Using advanced tree climbing techniques, we sampled one fully, sunlit canopy branch and, where it existed, a fully shaded branch, each at least 1 cm diameter, from each tree. Stems were fully bark-covered (not green). From each branch, we measured 1 to 2 leaves. Branches and leaves were chosen with minimal evidence of damage (i.e. herbivory). Xylem and leaf samples were placed in coolers for transport back to the lab, and were frozen before and after shipping before cryogenic

extraction. For plant water and wax hydrogen isotopic analyses, 176 individuals were sampled across 32 species and five forest plots across the Andean-Amazon gradient.

## 2.4. Plant water sampling

Leaf samples were collected in the early afternoon for water extractions and leaf wax analysis as described above by the CHAMBASA protocols. Leaves were cut at the base of the leaf, placed into glass vials and kept cool until analysis. Stem samples were also collected 30 cm below the leaf and similarly placed into glass vials for xylem water isotopic analyses.

Water was cryogenically extracted from the xylem and leaf samples (as described in Vendramini and Sternberg, 2007) for water isotopic analysis. After water extraction, the same leaf tissue was chopped and extracted for leaf wax isotopic composition reported here. Plant waters were analyzed by isotope ratio mass spectrometry (IRMS; Finnigan Mat DeltaPlus XL, Germany) at

analyzed by isotope ratio mass spectrometry (IRMS; Finnigan Mat DeltaPlus XL, Germany) at the UC Berkeley Center for Stable Isotope Biogeochemistry. The stable H isotope composition of all water samples was determined using the method outlined by Nelson and Dettman (2001); the stable O isotope composition was determined using a 5-day equilibration of water samples with  $CO_2$  followed by mass spectrometry analysis (Epstein and Mayeda 1953; Brooks and Dawson 2001). The external precision is better than 0.1% for  $\delta^{18}O$  and 0.8% for  $\delta D$ .

## 2.5. Lipid extraction

Dried, chopped plant leaves were immersed in dichloromethane (DCM):methanol (MeOH; 9:1 v/v) and agitated manually by pipette to extract plant waxes in solution. The extract was separated using column chromatography (5 cm x 40 mm Pasteur pipette, NH<sub>2</sub> sepra bulk packing, 60 Å), eluting with 2:1 DCM:isopropanol, followed by 4% HCO<sub>2</sub>H in diethyl ether,

yielding neutral and acid fractions respectively. The neutral fraction was separated by column chromatography (5 cm x 40 mm Pasteur pipette, 5% water-deactivated silica gel, 100–200 mesh) by eluting with hexanes to separate n-alkanes. The acid fraction containing n-alkanoic acids was transesterified with 5% HCl and 95% MeOH ( $\delta D_{\text{methanol}} = -198.3\% \pm 3.9$ ;  $\sigma$ ) at 70 °C for 12 hours to yield corresponding fatty acid methyl esters (FAMEs). Excess milliQ water was added to the hydrolyzed products, and the lipids were partitioned into hexane and dried by passing through anhydrous Na<sub>2</sub>SO<sub>4</sub>. Lipids were further purified using column chromatography (5 cm x 40 mm Pasteur pipette, 5% water-deactivated silica gel, 100–200 mesh), eluting with hexane first and then with DCM to isolate the pure FAME fraction.

## 2.6. Biomarker identification and quantification

We identified the *n*-alkanes and *n*-alkanoic acids (the latter as methyl esters) by gas chromatography mass spectrometry and quantified these compounds by a flame ionization detector relative to an in-house mixture of *n*-alkanes and *n*-alkanoic acid methyl esters of known concentration.

## 2.7. Compound-specific hydrogen isotopic analysis

Compound-specific hydrogen isotopic values were obtained using gas chromatography isotope ratio mass spectrometry (GC-IRMS). We used a Thermo Scientific Trace gas chromatograph equipped with a Rxi-5ms column (30 m x 0.25 mm, film thickness 1 µm) and a programmable temperature vaporizing (PTV) injector operated in solvent split mode with an evaporation temperature of 150 °C to exclude abundant C<sub>16</sub> and C<sub>18</sub> *n*-alkanoic acids, following Feakins et al. [2014]. The GC was connected via a GC Isolink with pyrolysis furnace (at 1400 °C) via a Conflo

IV interface to a DeltaVPlus isotope ratio mass spectrometer. To check for linearity, the  $H_3$  factor was measured daily and remained close to 4 ppm mV<sup>-1</sup> (across 1–8 V). Reference peaks of  $H_2$  were co-injected during the course of a GC-IRMS run; two were used for standardization. Samples were interspersed with standard compound mixtures of known isotopic composition. Data were normalized to the VSMOW/SLAP hydrogen isotopic scale by comparing with an external standard obtained from A. Schimmelmann, Indiana University, Bloomington, containing 15 *n*-alkane compounds ( $C_{16}$  to  $C_{30}$ ), with  $\delta D$  values spanning -9 to -254%. The RMS error determined by replicate measurements of the standard across the course of analyses was 4.2‰. Correction for H added by methylation of FAs as methyl esters was made by way of mass balance. The results are reported using conventional delta notation ( $\delta D\%$ ).

# 2.8. Isotopic fractionations

We compare the measured isotopic values of environmental waters, plant waters and biomarkers in order to calculate the enrichment factors associated with the various isotopic effects. We report isotopic fractionations between two measured substrates,  $\delta D_a$  and  $\delta D_b$ , as enrichment factors ( $\varepsilon_{a/b}$ ), calculated with the following equation:

320 
$$\varepsilon_{a/b} = \alpha_{a/b} - 1 = [(\partial D_a + 1)/(\partial D_b + 1)] - 1$$
 (1)

where a is the product and b is the substrate.  $\delta D$  and  $\varepsilon$  are reported here in per mil units (‰) which implies a factor of 1000 (Cohen et al., 2007). When reporting plant water isotopic fractionations, the superscript specifies the enrichment of the heavier isotope of hydrogen

 $({}^{2}\varepsilon_{LW/XW})$  or oxygen  $({}^{18}\varepsilon_{a/b}\,_{LW/XW})$ .

# 2.9. Community-weighted averaging of plant wax isotopic traits

Since waxiness of plant leaves varies, we weighted the isotopic composition for the concentration of each compound (concentration-weighted plot mean). To account for the variable contributions of species in a forest plot, we weighted for both wax concentration and abundance of each sampled species (community-weighted plot mean). Species proportional contributions were based on total basal area for each species and taxonomic inventories collected between 2009 and 2014, during which time there was no major disturbance (e.g. landslide, fire, deforestation) in these old growth forests. The weighted means and the weighted standard deviations were calculated using the general formula:

$$\bar{x}_{w} = \frac{\sum_{i=1}^{N} w_{i} \cdot x_{i}}{\sum_{i=1}^{N} w_{i}} \quad (2) \qquad \qquad \sigma_{w} = \sqrt{\frac{\sum_{i=1}^{N} w_{i} \cdot (x_{i} - \bar{x}_{w})^{2}}{(N-1) \cdot \sum_{i=1}^{N} w_{i}}} \quad (3)$$

where  $w_i$  is the weight for the i<sup>th</sup> observation, N is the number of non-zero weights, and  $\bar{x}_w$  is the weighted mean of the observations.

#### 3. RESULTS

## 3.1. Meteoric water isotopic composition

Biweekly precipitation samples from 4 sites across the elevation profile spanned 9/2/2013 to 7/23/2014. No samples were collected during the wet season at the high elevations, when heavy rain and landslides make access challenging. Dual isotopic analysis indicates a local meteoric water line (LMWL) of  $\delta D$  (‰) = 7.62 $\delta^{18}O$  + 4.30 (R<sup>2</sup> = 0.97; n = 45); (Fig. 2A). The LMWL from our biweekly sampling is similar to that reported for discrete precipitation samples in prior years from the Andean sector (Clark et al., 2014), as well as to the global meteoric water line (GMWL) relationship of  $\delta D$  (‰) =  $8\delta^{18}O$  + 10 (Craig, 1961). Deuterium excess, calculated as d

=  $\partial D - 8 * \delta^{18}O$ , has a mean value of 7‰ ( $\sigma$ = 6) from the biweekly samples. Biweekly precipitation samples displayed seasonality:  $\partial D$  values ranged over 100‰ at each elevation where year round collections were made (Appendix A). As sampling was not optimized for collecting precipitation amounts, and we do not have wet season sampling from the high elevation sites, we do not attempt to calculate mean annual precipitation isotopic compositions or regression with elevation.

345

346

347

348

349

350

351

352

353

354

355

356

357

358

359

360

361

362

363

364

365

366

Stream water  $\delta D$  values were reported in a prior publication (Ponton et al., 2014), which found the expected depletion of the heavier isotope with elevation with ordinary least squares regression of elevation against  $\delta D$  yielding a slope of -22% km<sup>-1</sup> (R<sup>2</sup> = 0.96, n = 24, dry season) and  $-17\% \text{ km}^{-1}$  ( $R^2 = 0.92$ , n = 15, wet season). Those stream water data are also here considered for their dual isotopic composition. We find stream waters fall within the error of the LMWL (stream  $\delta D \% = 8 \delta^{18}O + 15$ ; shown separated by season of collection in Fig. 2A). The slopes of the isotope-elevation relationship for  $\delta^{18}$ O are -2.75% km<sup>-1</sup> (R<sup>2</sup> = 0.94, n = 24, dry season) and -1.96% km<sup>-1</sup> respectively (R<sup>2</sup> = 0.92, n = 15, wet season). Stream water isotopic composition is identical in wet and dry seasons in the uplands, reflecting the residence time of baseflow from soils and fractured rock (Clark et al., 2014), whereas lowland streams vary seasonally by c. 20% in  $\delta D$  reflecting a buffered version of the seasonal cycle in the measured isotopic composition of precipitation. We thus find that stream waters average out short-term variability in precipitation, fall on the LMWL and show expected depletion in the heavier isotopes with elevation (Fig. 2A). The stream waters thus substantiate the precipitation sampling, providing a practical means to establish the meteoric water isotopic composition available to plants during brief fieldwork visits to remote settings.

## 3.2. Plant xylem water isotopic compositions

We find a -18 to -186% range in the hydrogen isotopic composition of plant xylem waters  $(\partial D_{XW})$  and -3 to -30% range in oxygen isotopes  $(\partial^{18}O_{XW})$ . The slope of the regression of  $\partial D_{XW}$  and  $\partial^{18}O_{XW}$  with elevation is -21% km<sup>-1</sup> (R<sup>2</sup> = 0.85, n = 156) and -3.90% km<sup>-1</sup> respectively (R<sup>2</sup> = 0.63, n = 117). Scatter between samples is likely due to temporal and spatial variability in plant water uptake between individuals and species. Xylem waters generally fall near the LMWL, with some notably above the LMWL at ESP-01 (Fig. 2). These xylem water values above the LMWL are indicative of atmospheric vapor sources, and are in part consistent with the range of values for cloud water reported by a prior study (Clark et al., 2014; Horwath, 2011). Those cloud water values are shown on Fig. 2, representing sampling from  $\sim$ 5 collections at 5 elevations between 1500 and 3600 masl during the dry season only. We would expect more depleted precipitation and cloud water at times and this may explain the observed stem water values. Few xylem water values fall below the LMWL, indicating evaporatively-enriched soil water is not a factor here.

## 3.3. Leaf water isotopic composition

In three sites, ESP-01, TAM-05 and TAM-06, leaf waters are D-enriched above xylem water (Fig. 3) and dual isotopic analysis reveals that they fall below the LMWL, indicating leaf water evaporative enrichment (Fig. 2B). However, at SPD-01 and SPD-02, leaf waters and xylem waters are indistinguishable or more D-depleted than xylem waters and fall on the LMWL. Using Eqn. 1, we calculate the 'leaf water enrichment,' i.e., the enrichment of bulk leaf water (LW) over xylem water (XW) for both hydrogen ( ${}^2\varepsilon_{\text{LW/XW}}$ ) and oxygen ( ${}^{18}\varepsilon_{\text{LW/XW}}$ ). Leaf water enrichment averages 15% ( $\sigma = 22$ , n = 72) and 5.9% ( $\sigma = 5.9$ , n = 52) for  ${}^2\varepsilon_{\text{LW/XW}}$  and  ${}^{18}\varepsilon_{\text{LW/XW}}$  respectively across the entire transect. In the lowland tropical forest sites in this study, measured

 $^{2}\varepsilon_{\text{LW/XW}}$  is small, with a mean value of +6‰ ( $\sigma$  = 6, n = 52), and negligible at the wettest SPD-01 and SPD-02 sites at c. 1.5 km asl and highest at the upper site +29‰ ( $\sigma$  = 25, n = 18). This points to MAP and RH as the dominant variable in determining  $\varepsilon_{\text{LW/XW}}$  across the elevation profile, consistent with global patterns (Sachse et al., 2012). We find no significant difference between sun and shade leaves overall, indicating that other environmental or plant physiological factors are more important for leaf water enrichment than sun exposure.

## 3.4. Leaf wax molecular concentrations

We report the compound-specific concentration of the n-alkane and n-alkanoic acid homologues for each individual plant sample (Appendix A). n-Alkanes are generally more concentrated than n-alkanoic acids. The  $C_{29}$  n-alkane has the highest concentration with a mean abundance of 113  $\mu g g^{-1}$  whereas the  $C_{30}$  n-alkanoic acid has a mean of 34  $\mu g g^{-1}$ . Concentrations range over an order of magnitude and in some individuals n-alkanoic acid concentrations are too low for isotopic determination.

#### 3.5. Leaf wax hydrogen isotopic compositions

We measured compound-specific  $\delta D_{\text{wax}}$  values for a total of 176 plant samples from 32 different species and found  $\delta D_{\text{wax}}$  values that range from -102 to -278 ‰ across all measured compound classes, species and sites (Appendix A). Linear regression of the  $\delta D$  values for  $C_{24}$  to  $C_{32}$  n-alkanoic acids and  $C_{27}$  to  $C_{31}$  n-alkanes indicate strong relationships between all compounds ( $R^2 > 0.9$ ), with the exception of the  $C_{32}$  n-alkanoic acid that is restricted to the lower elevation sites. We find the  $\delta D$  values of n-alkanoic acids and n-alkanes correlate well with xylem water (Fig. 4a, b). There is no significant correlation with bulk leaf waters (Fig. 4c, d), which fall in two

410 clusters, with enriched waters at the lowland (TAM-05 and TAM-06) and upland (ESP-01) sites and non-enriched waters at the wettest sites (SPD-01 and SPD-02). 411 Using Eqn. 1 we calculate the apparent fractionation between  $\delta D$  values of source water and 412 wax. We consider both (1) site mean estimates of source water based on the plot elevation and 413 the ordinary least squares regression-based estimate of stream water measured values for that 414 415 elevation (w), as well as (2) the directly measured xylem water from individual plants. Since  $\delta D_{XW}$  is similar to  $\delta D_{W}$  we also find that the unweighted mean fractionations for these 416 individuals using stream water or xylem waters are the same within uncertainties:  $\varepsilon_{28\text{acid/w}} = -121$ 417  $\pm 31 \%$  ( $\sigma$ , n = 102) versus  $\varepsilon_{28acid/XW} = -128 \pm 31 \%$  ( $\sigma$ , n = 83) and  $\varepsilon_{29/w} = -129 \pm 22 \%$  ( $\sigma$ , n = 83) 418 419 136) versus  $\varepsilon_{29/\text{XW}} = -136 \pm 21 \%$  ( $\sigma$ , n = 111; with smaller sample sizes for  $\varepsilon_{\text{wax/XW}}$  due to loss 420 of some xylem water samples). We further find no significant difference in apparent

fractionation between sun and shade leaves by Student's t test, indicating that source water (w)

and other environmental or plant physiological factors are more important than sun exposure.

421

422

#### 4. DISCUSSION

424

425

426

427

428

429

430

431

432

433

434

435

436

437

438

439

440

441

442

443

444

445

## 4.1. Ecohydrology and implications for plant wax $\delta D$

Only a few studies have compared  $\delta D$  values of plant waters with those of plant biomarker molecules across natural environmental transects (e.g., Feakins and Sessions, 2010; Kahmen et al., 2013b; Tipple and Pagani, 2013), and none have done so in a very wet tropical ecosystem. In this study, we add dual isotope analyses of plant waters to add further insights into resolving water sources. We directly sampled xylem waters to establish plant water sources and find that most xylem waters fall on the LMWL with minimal deviations (Fig. 2), indicating precipitation as the major source of water. Some xylem waters fall above the LMWL at the highest TMCF site (ESP-01). These xylem water values may be indicative of atmospheric vapor sources and are in part consistent with the range of values for cloud water and shown on Fig. 2, representing sampling from ~5 collections at 5 elevations between 1500 and 3600 masl during the dry season only (Clark et al., 2014; Horwath, 2011). We would expect more depleted precipitation and cloud water at times (extrapolating the sampled range) and this may in part explain the few stem water values that fall beyond the available cloud water dataset. As persistent cloud reaching ground level immerses the area (Halladay et al., 2012), we infer that plants are accessing fog inputs to soils, a phenomenon previously documented in TMCF (Eller et al., 2013). We can also establish whether plant source waters are well characterized by the isotopic composition of mean annual precipitation or whether they vary among precipitation events. We find that xylem waters have much less scatter than 2-week integrated precipitation collections that range in  $\delta D$  values by over ~100% at each site. Instead xylem water isotopic compositions fall close to that of stream water. Stream water is composed of annually-integrated precipitation

stored in soil and fractured rock in the Andes (Clark et al., 2014) and seasonally-integrated meteoric water in the lowland rainforest (Ponton et al., 2014). We infer that xylem water is relatively insensitive to shorter-term variations in precipitation isotopic composition, and that plants are generally accessing water stored in soil and fractured rock. Overall we find a minor enrichment of leaf water above xylem water.  ${}^2\varepsilon_{LW/XW}$  averages  $+15\pm2$ % (s.e.m., n = 72) confirming leaf water model projections for the tropics (Kahmen et al., 2013a; West et al., 2008). The suppression of leaf water enrichment results from equilibration of leaf water with atmospheric water vapor at high RH via exchange through the stomata (Farquhar et al., 2007) and in the TMCF via foliar uptake of precipitation accumulated on leaf surfaces (Eller et al., 2013; Goldsmith et al., 2013) (illustrated in Fig. 5). However, the weak correlation between  $\delta D_{LW}$  and  $\delta D_{wax}$  (Fig. 4c, d) leads us to infer that the bulk leaf water, as sampled in the afternoon in the dry season (May-October), is not representative of the substrate for biosynthesis of the lipids. Therefore, we suggest caution in interpreting  $\varepsilon_{\text{wax/LW}}$ , the fractionation between  $\delta D_{wax}$  and bulk leaf water as calculated from this study, as we have likely not captured the fractionation relevant to determining  $\varepsilon_{bio}$ . Leaf water varies in isotopic composition on a diurnal and seasonal basis (Li et al., 2006), and spatially within the leaf from the xylem water supply to the enriched water near stomata. Leaf water and leaf waxes were sampled at the same time, but the waxes would have been synthesized from leaf waters at an earlier time, likely soon after leaf formation (Tipple et al., 2013). In the tropics, leaves are formed year round with a slight increase

in September during the dry season (Malhi et al., 2014a). Given spatiotemporal variation in leaf

water isotopic composition, measured bulk leaf water may not relate to the substrate used for

synthesis of leaf waxes. For the purpose of understanding the physical controls on the  $\delta D$  of

446

447

448

449

450

451

452

453

454

455

456

457

458

459

460

461

462

463

464

465

466

plant leaf waxes, we therefore rely upon the  $\delta D_{XW}$  (xylem water, Fig. 4a, b) or the  $\delta D_{w}$  (i.e. stream water as an integrated measure of precipitation). The main water fluxes are schematically illustrated as relevant for leaf wax hydrogen isotope systematics in Fig. 5.

## 4.2. The fractionations between meteoric waters and plant leaf waxes

468

469

470

471

472

473

474

475

476

477

478

479

480

481

482

483

484

485

486

487

488

The net or apparent fractionation ( $\varepsilon_{app}$ ) between water and wax is the most commonly reported fractionation (Fig. 5), where water is typically mean annual precipitation isotopic composition, often derived from interpolations of sparse observational data. In order to establish whether leaf wax biomarkers record local meteoric water isotopic composition, we measured plant water and wax isotopic composition and directly determined fractionations at the individual tree level. Overall, we find  $\varepsilon_{\text{wax/w}}$  (i.e. here measured directly between source water and leaf wax) for  $C_{28}$  nalkanoic acids to be  $-121 \pm 3\%$  (s.e.m, with 31%  $\sigma$ , n = 102; Fig. 6c) and for  $C_{29}$  n-alkanes to be  $-129 \pm 2\%$  (s.e.m, with 22%  $\sigma$ , n = 136; Fig. 6d). In this ecosystem, we find that  $\varepsilon_{\text{wax/w}}$  and  $\varepsilon_{\text{wax/XW}}$  are indistinguishable within uncertainties overall, indicating that the variability of plant waters from stream water values is no larger than variability associated with biosynthesis. The picture of hydrogen isotope systematics that emerges is as follows. In this very wet tropical ecosystem, with 2–5 m of rainfall per year, precipitation inputs to soil and rock storage average out variability between storms (Clark et al., 2014) and the water that is either stored, exported in small stream flow or accessible to plants is isotopically indistinguishable. This finding confirms the validity of using measured small stream water values in place of plant water sampling or precipitation isotope collections that are hard to maintain in remote regions. Notably, we find that the leaf wax proxy operates along this moist tropical elevation transect with only a

negligible contribution from the leaf water enrichment as predicted in a prior modeling study (Kahmen et al., 2013a).

These fractionations are consistent with those reported in humid areas globally (Sachse et al., 2012), for example  $\varepsilon_{\text{wax/w}}$  in these tropical forests is no different from those reported for a humid, temperate forest in Massachusetts, USA (Hou et al., 2007). In that temperate forest  $\varepsilon_{\text{wax/w}}$  for the C<sub>29</sub> n-alkane was  $-130 \pm 4\%$  (standard error of the mean, s.e.m., n = 35), calculated relative to interpolated precipitation isotope estimates (Hou et al., 2007), similar to the value we found for this Peruvian tropical forest ( $-129 \pm 2\%$  s.e.m., n = 136) relative to measured environmental waters. Given the difference in sample size and different or unknown sampling strategies, the variance cannot be quantitatively or qualitatively evaluated between the two studies. The key findings are that we do not find that megadiverse tropical rainforests present particular obstacles to leaf wax proxy reconstructions, and we find the same  $\varepsilon_{\text{wax/w}}$  fractionations in both temperate and tropical forests.

Within our study we did however find that the range of  $\varepsilon_{\text{wax/w}}$  variability was larger at the Andean sites (SPD-02 and above) than in lowland rainforest sites. The range of fractionations at the individual plant level is interesting, as it includes some surprisingly small fractionations in the very wet tropical montane climatic environment. Fractionations <-100% have previously only been reported from locations with <2 m yr<sup>-1</sup> precipitation (Sachse et al., 2012), including locations with an order of magnitude less MAP (Feakins and Sessions, 2010) than in our study sites in Peru. Here we find a large number of individuals with  $\varepsilon_{\text{wax/w}}$  <-100% (**Fig. 6**), in very wet climates with 5 m yr<sup>-1</sup> precipitation. We hypothesize that foliar water uptake in the TMCF may sometimes result in smaller than expected  $\varepsilon_{\text{wax/w}}$ . Intriguingly, fractionations at SPD-01 are

smaller than at SPD-02 (especially for the n-alkanoic acids); these are two neighboring sites that differ in fog inundation falling above and below the cloud base respectively (Halladay et al., 2012). This pattern would be consistent with foliar uptake of fog waters in cloud forests (Goldsmith et al., 2013; Gotsch et al., 2014), but this hypothesis was not supported by our one-time sampling of leaf water in this study. Instead we found  $\partial D_{LW}$  lower than  $\partial D_{XW}$  values (Fig. 3), perhaps reflecting a single D-depleted precipitation and foliar uptake event. While we suspect that source water variability in cloud forests may introduce isotope effects, we cannot explain these plant water observations satisfactorily with available data at this time. Diurnal and seasonal plant water sampling (Gotsch et al., 2014) paired with leaf wax analysis, or experimental studies, could document how foliar uptake in the TMCF may introduce isotope effects in plant leaf waxes, in order to determine the physiological or biochemical basis of the small fractionations observed in a few species. Overall, these species appear to be outliers and we do not find a significant difference in the central estimate of fractionations for upland tropical forests compared to that of lowland tropical forests in this study, or from those of temperate forests.

#### 4.3. Comparison of *n*-alkanes and *n*-alkanoic acids

Both n-alkanes and n-alkanoic acids are commonly employed in leaf wax biomarker studies; however, few calibration studies have provided data for multiple compound classes. From 176 plant samples that include 32 different species in our Peruvian tropical forest transect, comparing compound classes, we found similar regressions of  $\delta D_{\text{wax}}$  as a function of elevation (Fig. 3), and similar relationships of  $\delta D_{\text{wax}}$  as a function of xylem water across all chain lengths (Fig. 4a, b). Our new results augment data from temperate sites in Japan (Chikaraishi and Naraoka, 2007) and from Massachusetts, USA (Hou et al., 2007); both those prior studies indicated that n-alkanes

were depleted by up to 30% relative to n-alkanoic acids. Long chain alkyl lipids are synthesized from the addition of 2 carbon acid groups to yield long chain n-alkyl acyl-ACP of carbon chain length n, forming even chain length n-alkanoic acids also of length n, as well as n-alkanes of n-1 (Chikaraishi and Naraoka, 2007; Zhou et al., 2010). We therefore compare pairs of C<sub>n</sub> n-acid and  $(C_{n-1})$  *n*-alkane to assess the isotopic fractionation associated with the decarboxylation process and any resulting compound class offset that would be relevant for paleoclimate applications. For some individuals we have  $\delta D_{\text{wax}}$  values for both the  $C_{30}$  *n*-alkanoic acid and the  $C_{29}$  *n*-alkane, and we found a mean D-depletion of the *n*-alkane by -3% ( $\sigma = 17\%$  for a sample size of 64 individuals from 16 different species). Neither the mean nor median of  $\varepsilon_{30acid/w}$  and  $\varepsilon_{29/w}$ fractionations significantly differed by Student's t test. Comparison of other pairs of acid and alkane of chain length (i.e., n and n-1 pairs) yield similar results. This is in contrast to the two prior studies that found an offset between compound classes and we suggest the difference may perhaps be a function of the small sample sizes in those prior studies. In these tropical trees we found species with compound class offsets on the order of  $\pm 30\%$  as well as individuals and species that showed little offset, leading to the overall compound class offset being insignificant. We speculate that the differences in compound class offsets that we observed in some species may arise due to biosynthetic differences in the production of each compound class between species, such as temporal offsets and use of stored carbohydrates; as the lack of overall, consistent difference does not support prior hypotheses of a large fractionation associated with decarboxylation. We note that in sedimentary records offsets between compound classes may arise for additional reasons such as polarity (affecting aqueous or sedimentary affinity) or lability.

533

534

535

536

537

538

539

540

541

542

543

544

545

546

547

548

549

550

551

552

553

These data would tend to support the use of the *n*-alkanes over the *n*-alkanoic acids as proxy records based on a couple of observations. 1) We observe greater variability in the *n*-alkanoic acid isotopic values than among the *n*-alkanes. For example, site-to-site variability in  $\varepsilon_{28\text{acid/w}}$  ( $\sigma$ = 40%; Fig. 6c) is double that for  $\varepsilon_{29/w}$  ( $\sigma$  = 19%; Fig. 6d). 2) In addition, *n*-alkanes are more abundant in most sampled individuals (Appendix A). Thus on both counts we infer that nalkanes may be more robust recorders of precipitation isotope signals in living tropical trees and tropical ecosystems. However we note that *n*-alkanoic acids confer advantages and have been often applied in sedimentary systems (Galy et al., 2011; Ponton et al., 2014), whether because of concerns over petrogenic inputs of *n*-alkanes (Pearson and Eglinton, 2000) or because of higher abundances of *n*-alkanoic acids, perhaps as a result of better packaging and preservation in sediments. Consideration of the utility of compound classes should consider living vegetation (which may favor a focus on *n*-alkanes), as well as sedimentary transformations and application (which may favor a focus on *n*-alkanoic acids). Choice of the target chain length may often practically be constrained by relative abundance, interference on the chromatogram and consideration of sources, however we show here, that in plants themselves, all reported nalkanoic acid and *n*-alkane chain lengths record the primary  $\delta D_{XW}$  signal (Fig. 4a, b).

## 4.4. Community-averaged plant wax isotopic compositions

555

556

557

558

559

560

561

562

563

564

565

566

567

568

569

570

571

572

573

574

575

When calculating community-averages we must account for the fact that individual plants vary not only in their compound-specific isotopic composition but also in the amount of individual leaf wax compounds produced. We thus scale isotopic measurements and fractionations by wax concentration at the individual level (Fig. 6a, b, 7a, b), an approach that has been also suggested

in a study of African ecosystems (Garcin et al., 2014) and we report concentration-weighted means for each site (Fig. 6c, d, 7c, d).

576

577

578

579

580

581

582

583

584

585

586

587

588

589

590

591

592

593

594

595

596

Species also vary in their dominance within the plant community. We further report the community-weighted mean leaf wax isotopic compositions and fractionations, i.e. a central estimate that accounts for both the different concentration of leaf waxes (on a compound-specific basis) and the relative abundance of each species in the forest plot (based on basal area) yielding the 'community-weighted' mean, our best estimate (Fig. 6c, d, 7c, d). The total proportion of the community represented by our sampling is illustrated on a site-by-site basis (Fig. 6e). Sites with low representation are more likely to have offsets between estimates of the mean with different weighting schemes and are more likely to have biased estimates of the mean based on small sample sizes (e.g., SPD-01). Apparent fractionations can be directly compared across all sites and we find surprising agreement in the central estimates across the transect. We find that the overall mean and  $\sigma$  of all individuals encompasses the central values for all sites (Fig. 6c, d); thus we find no significant bias in apparent fractionations along the elevation profile. Given the lack of systematic variation in apparent fractionation, community-weighted mean  $\delta D_{\text{wax}}$  responds to elevation with a slope of  $-17\% \text{ km}^{-1}$  for the *n*-alkanoic acids and  $-18\% \text{ km}^{-1}$ for the *n*-alkanes (Fig. 7c, d). These slopes carry error associated with the standard errors of site means, as well as unquantifiable uncertainty associated with the small number of sites, and low proportion of community representation (illustrated on Fig. 6). Thus, the errors on the slopes are

poorly constrained but are assumed to be greater than site uncertainties and therefore > 5% km<sup>-1</sup>.

The altitude effect in meteoric water, as sampled by stream waters, displays gradients of -22%

km<sup>-1</sup> in the dry season and –17‰ km<sup>-1</sup> in the wet season. Within uncertainties, we conclude that the isotope-elevation slopes for wax are equivalent to that of meteoric water.

597

598

599

600

601

602

603

604

605

606

607

608

609

610

611

612

613

614

615

616

617

618

For the *n*-alkanoic acids, the mean value for site SPD-01 appears as an outlier from the linear trend defined by the other 4 sites, as illustrated by comparing this sites inclusion and removal from the dataset (Fig 7c). The proportion of the community represented by our sampling at this site may be insufficient to characterize accurately the site mean value, as this value is based upon only 4 species that comprise just 2% of total basal area (Appendix A). Our failure to sample adequately at SPD-01, is expected to introduce accuracy errors into our central estimate for this site (Paine et al., 2015) and emphasizes the need for large sample sizes and/or assessments of representation. Overall our sampling yielded leaf wax  $\delta D$  results with sample sizes per hectare plot comprising 11-32 samples from 3-8 species (i.e., fewer than sampled, given low nalkanoic acid concentrations in some samples). The sampled species represent 23 - 406 stems (total number of stems of sampled species) and 2 - 53% of basal area in each forest plot (Appendix A). We identified the predicted relationship with elevation for the communityweighted mean  $\delta D$  values of the *n*-alkanes (Fig. 7). Although our sampling may not be sufficient to rule out accuracy errors associated with sample means being biased estimates of population means, the census counts allow us to quantify how representative the samples are and to evaluate appropriate strategies for future work.

As our sampling targeted prevalent species, the community-weighted mean estimates for both  $\varepsilon_{\text{wax/w}}$  (Fig. 6) and leaf wax  $\delta D$  (Fig. 7) are not significantly different from the unweighted sample mean within uncertainties. This may be taken as indication that community-weighting is not necessary, but, we caution that if studies target species without attention to dominance, then

community-weighting may be more critical. In particular, studies that sample across phylogenetic diversity and consequently include species that are either functioning very differently (e.g. water uptake, seasonality of growth) or biosynthesizing differently (e.g. varied use of stored carbohydrates) we would expect isotope effects. For example, rare species occupying distinct niches may have functions that differ from dominant species.

In summary, sampling guided by community-representation should be a robust approach to calibration in all ecosystems. In tropical rainforests, collecting large sample sizes and focusing on common species is recommended to understand landscape-scale biogeochemical signatures. Community-weighting may be more important at sites of low diversity and high dominance, such as alpine grasslands (Lavorel et al., 2008), where a few species may exert a strong influence on the central estimate by having a unique water uptake or biosynthesis strategy.

# 4.5. General implications for paleoclimate applications

This comprehensive study of hydrogen isotope systematics in tropical lowland and montane rainforests provides modern observational data to support tropical paleoclimate reconstructions. Strong correlations ( $R^2 = 0.97$ ) between  $\delta D_w$  and community-averaged  $\delta D_{wax}$  values support application of the leaf wax hydrogen isotope proxy for paleoprecipitation (Fig. 8). This study constitutes the first major calibration of hydrogen isotopes systematics – environmental waters, plant waters and plant leaf wax – in tropical forest ecosystems. Model predictions of minimal leaf water isotopic enrichment (<20‰) in tropical forests including Amazonian forests (Kahmen et al., 2013b) are confirmed here with  ${}^2\varepsilon_{LW/XW}$  mean enrichment of  $+15\pm2\%$  (s.e.m., n=72). We do not find substantive differences between mean  $\varepsilon_{wax/w}$  for the  $C_{29}$  n-alkanes for these

tropical forests (c. -129%) and prior data collection in multiple studies for C<sub>3</sub> trees (c. -121%) from extratropical locations (Sachse et al., 2012). We also find no significant overall offset between n-alkanes and n-alkanoic acids, in contrast to prior reports, and therefore combine both compound classes in regression of  $\delta D_{\text{wax}}$  on  $\delta D_{\text{w}}$  (Fig. 8). These calibrations justify using a value of  $\varepsilon_{\text{wax/w}}$  value of c. -130% when reconstructing paleoprecipitation  $\delta D$  values in tropical forests, and indeed all moist forest environments. Proxy uncertainties derive from multiple factors, many of which are incompletely quantified, but overall are likely >10‰ and this impacts the precision and accuracy of paleoprecipitation reconstructions. Importantly, we find no  $\varepsilon_{\text{wax/w}}$  change along a fully-forested transect with high alpha and beta diversity, suggesting that tropical reconstructions will also be robust to species turnover so long as ecosystems remain forested over geological time.

Based on global calibration efforts across climate systems and ecosystems, the main complications for the leaf wax  $\delta D$  proxy arise when a) shifting into dry climates, which entail smaller apparent fractionations of up to c. -90% due to leaf water enrichment or b) shifting to grassland ecosystems with attendant larger fractionations up to c. -150% due to leaf physiology (Sachse et al., 2012). Although dry woody, subtropical ecosystems in California were found to exhibit smaller fractionations c. -90%, no sensitivity to the gradient in MAP and RH was detected across that aridity transect, presumably because of varied plant adaptive responses to climate (Feakins and Sessions, 2010). Identifying the transition between wet and dry ecosystems and thus knowing which fractionation to apply is important for paleo-applications. Global compilations indicate that the transition appears to occur around 600 mm a<sup>-1</sup> precipitation and <0.65% mean relative humidity (Sachse et al., 2012). In order to detect such transitions and to

yield paleoprecipitation isotope reconstructions that are robust to these climatic and ecological changes, applications of the leaf wax proxy would benefit from multi-proxy reconstruction with other moisture proxies, e.g., grain size for runoff or pollen for plant community assemblages (Dingemans et al., 2014), in order to resolve whether a shift in fractionation is likely across the reconstruction period. Such studies would yield both wet-dry and precipitation isotope reconstructions adding value to climate interpretations. In addition, pollen reconstructions of plant types, and in particular grass %, are useful complements to leaf wax  $\delta D$  measurements towards robust paleoprecipitation  $\delta D$  reconstructions (Feakins, 2013).

Replication of calibration efforts in other tropical forests, e.g. central Africa and southeast Asia, remains an important test, given the taxonomic differences of tropical forests that may incur hydrogen isotope effects associated with biosynthesis. In those other major tropical forest systems additional forest plot calibration studies would help to secure application of the proxy elsewhere. As part of systematic efforts to specifically assess taxonomic differences (rather than community/landscape averages), phylogenetic sampling schemes may replace forest plot approaches. Phylogenetic studies (Diefendorf et al., 2011; Diefendorf et al., 2015; Gao et al., 2014) have begun to assess systematic genetic bases for plant wax trait variations and fractionation differences. In phylogenetic studies, we recommend sampling with attention to phylogenic position and adequate representation in that case pertains to the number of samples per phylogenetic branch as well as to sampling the full range of environments in which those taxa are found in order to separate environmental effects from taxonomic effects. Whatever the approach to calibration and study of modern ecosystems, there remain limitations in geological application. We must remember that widening the scope of modern calibration cannot fully

constrain uncertainties in the past due to plant adaptation and evolution, except in rare cases where plant leaf waxes as well as other archives of precipitation isotopes co-occur and allow paleo-calibration determinations of leaf wax fractionations (Porter et al., 2016).

In terms of additional calibration needs for tropical applications of the leaf wax  $\delta D$  proxy we highlight 3 key areas. 1) Further calibration work extending into seasonally dry tropical forests and mixed savanna ecosystems should be a priority for enabling robust paleoprecipitation isotope reconstructions across wet-dry climate shifts in the tropics. 2) Systematic studies of tropical hydrological processes might include observational or manipulation studies of foliar uptake in cloud forests in order to assess impacts on leaf wax  $\delta D$  values. 3) Additional unanswered questions pertain to tropical seasonality: although temperature seasonality is minimal compared to higher latitude climates, there is light seasonality even in low latitudes, including that associated with cloud cover (Halladay et al., 2012). In this ecosystem, there is a dry season (September) increase in new leaves, although leaf production continues year-round (Malhi et al., 2014a). In temperate zones, a spring bias in leaf growth and wax production indicates the seasonal nature of the temperate forest leaf wax recorder (Tipple et al., 2013). While we find a correlation between  $\delta D$  wax and year-round precipitation isotopes, it remains an open question for timeseries research as to whether tropical leaf waxes are year-round integrators. If there is any seasonal bias, we would predict preferential recording in the dry season, due to lighttriggered leaf flush, but we anticipate a more annually-integrative proxy in tropical applications than elsewhere.

#### 5. CONCLUSIONS

684

685

686

687

688

689

690

691

692

693

694

695

696

697

698

699

700

701

702

703

We have conducted a multi-species calibration of the leaf wax  $\delta D$  proxy in plant waters and environmental waters across an elevation gradient extending from tropical lowland rainforest to montane cloud forest ecosystems. Our survey supports the use of leaf wax biomarkers as paleohydrological proxies in the tropics. In particular, we find that the community-weighted mean wax isotopic compositions primarily record variations in the isotopic compositions of meteoric waters, thus validating the use of leaf wax biomarker hydrogen isotopic compositions to reconstruct paleohydrology in tropical forests. We find that the hydrogen isotopic composition of plant leaf waxes reflects that of precipitation after a larger biosynthetic fractionation as observed globally (Sachse et al., 2012), but that in high relative humidity atmospheres they are less affected than other ecosystems by the secondary isotope effects associated with leaf water enrichment, simplifying the application of this proxy to reconstruct the hydrogen isotopic composition of precipitation in wet tropical climates. We can reject our hypothesized link between high biodiversity and variable fractionations, such as might be expected if species and functional diversity in plant communities entails using differing growth strategies, including differing seasonality or use of stored carbohydrates. Instead we find the lowland rainforest does not display greater isotopic variability than other ecosystems. Furthermore, low dominance in such ecosystems means that no one species exerts a very large effect on ecosystem mean values. Instead, we identify more potential for biased estimates in the TMCF where dominance is higher, and where water sources include both precipitation and fog. Our plot-based transect provides an ecologically- and spatially-representative sampling approach across tropical lowland rainforest and montane cloud forests to characterize landscape-scale plant traits, and offer a window into the living assemblage of leaf wax traits for comparison to the molecular fossils in sediments that represent an archive of past ecosystems and environments.

705

706

707

708

709

710

711

712

713

714

715

716

717

718

719

720

721

722

723

724

725

726

# Acknowledgements

729	Contributing authors are part of the Andes Biodiversity and Ecosystems Research Group
730	ABERG (andesresearch.org), the Global Ecosystems Monitoring (GEM) network
731	(gem.tropicalforests.ox.ac.uk) and the Amazon Forest Inventory Network RAINFOR
732	(www.rainfor.org) research consortia. The field campaign was funded by grants to YM from the
733	UK Natural Environment Research Council (Grants NE/D01025X/1, NE/D014174/1), with
734	additional support from European Research Council advanced investigator grants GEM-TRAITS
735	(321131) and T-FORCES (291585) as well as the Jackson Foundation to YM and a John D. and
736	Catherine T. MacArthur Foundation grant to GA. GA and the spectranomics team were
737	supported by the endowment of the Carnegie Institution for Science, and by the National Science
738	Foundation (DEB-1146206), supporting the taxonomic contributions to the project. Carnegie
739	Airborne Observatory data collection, processing and analyses were funded solely by the John D.
740	and Catherine T. MacArthur Foundation. The Carnegie Airborne Observatory is supported by the
741	Avatar Alliance Foundation, John D. and Catherine T. MacArthur Foundation, Andrew Mellon
742	Foundation, David and Lucile Packard Foundation, Mary Anne Nyburg Baker and G. Leonard
743	Baker Jr., and William R. Hearst III. Laboratory work at USC was in part supported by the US
744	National Science Foundation (EAR-1227192) and the ACS Petroleum Research Fund (53747-
745	ND2) to SF. We thank the Servicio Nacional de Áreas Naturales Protegidas por el Estado
746	(SERNANP) and personnel of Manu and Tambopata National Parks for logistical assistance and
747	permission to work in the protected areas. We also thank the Explorers' Inn and the Pontifical
748	Catholic University of Peru (PUCP), as well as Amazon Conservation Association for use of the
749	Tambopata and Wayqecha Research Stations, respectively. Many researchers were involved in
750	the field, in particular we would like to thank E. Cosio, W. Huaraca-Huasca and J. Huaman for

- advising on field logistics; tree climbers: C. Costas, D. Chacón, H. Ninatay; field project
- supervision: T. Boza, M. Raurau; species identification and basal area: W. Farfan, F. Sinca; leaf
- areas R.M. Castro, G. Rayme, A. Robles, Y. Choque and Y. Valdez; and precipitation isotope
- 754 collections: T. Gonzalez, Amazon Center for Environmental Education and Research in Puerto
- 755 Maldonado; A. Whitworth, CREES at Manu Learning Center and N. Schulz, PUCP at SP and
- 756 WAY. We thank USC undergraduate lab assistants: C. Hua, K. McPherson, E. Rosca and A.
- Figueroa, as well as M. Rincon. This manuscript was improved with the comments of 3
- anonymous reviewers and Associate Editor Alex Sessions.

#### 759 APPENDIX A. SUPPLEMENTARY DATA

- Supplementary data associated with this article can be found, in the online version, at
- http://dx.doi.org/10..... The data include interactive Google Earth maps of the sampling locations
- as well as an Excel file containing all data reported described in this article.

#### 763 References

- Asner, G.P., Llactayo, W., Tupayachi, R., Luna, E.R. (2013) Elevated rates of gold mining in the
- Amazon revealed through high-resolution monitoring. *Proc. Nat. Acad. Sci. U.S.A* **110**, 18454–
- 766 18459.
- Bai, Y., Fang, X.M., Gleixner, G. and Mugler, I. (2011) Effect of precipitation regime on delta D
- values of soil n-alkanes from elevation gradients Implications for the study of paleo-elevation.
- 769 *Org. Geochem.* **42**, 838–845.
- Bai, Y., Fang, X.M., Jia, G.D., Sun, J.M., Wen, R. and Ye, Y.Q. (2015) Different altitude effect
- of leaf wax *n*-alkane delta D values in surface soils along two vapor transport pathways,
- southeastern Tibetan Plateau. *Geochim. Cosmochim. Acta* **170**, 94–107.
- Becker, A., Korner, C., Gurung, A.B. and Haeberli, W. (2007) Selected issues from the Samedan
- GLOCHAMORE workshop on altitudinal gradient studies. *Mt. Res. Dev.*. **27**, 82–86.

- Bruijnzeel, L.A., Mulligan, M. and Scatena, F.N. (2011) Hydrometeorology of tropical montane
- cloud forests: emerging patterns. *Hydrol. Process.* **25**, 465–498.
- 777 Chikaraishi, Y. and Naraoka, H. (2007) delta C-13 and delta D relationships among three n-alkyl
- compound classes (n-alkanoic acid, *n*-alkane and *n*-alkanol) of terrestrial higher plants. *Org.*
- 779 *Geochem.* **38**, 198–215.
- 780 Clark, K.E., Torres, M.A., West, A.J., Hilton, R.G., New, M., Horwath, A.B., Fisher, J.B., Rapp,
- J.M., Robles Caceres, A. and Malhi, Y. (2014) The hydrological regime of a forested tropical
- Andean catchment. Hydrol. Earth Syst. Sci. 18, 5377–5397.
- Cohen, E.R., Cvitaš, T., Frey, J.G., Holmström, B., Kuchitsu, K., Marquardt, R., I. Mills, F.P.,
- Quack, M., Stohner, J., Strauss, H.L., Takami, M. and Thor, A.J. (2007) Quantities, Units and
- 785 Symbols in Physical Chemistry, 3rd. Ed. Royal Society of Chemistry Publishing, Cambridge,
- 786 UK, pp. 265.
- Condit, R., Pitman, N., Leigh, E.G., Chave, J., Terborgh, J., Foster, R.B., Nunez, P., Aguilar, S.,
- Valencia, R., Villa, G., Muller-Landau, H.C., Losos, E. and Hubbell, S.P. (2002) Beta-diversity
- 789 in tropical forest trees. Science **295**, 666–669.
- 790 Cox, P.M., Betts, R.A., Collins, M., Harris, P.P., Huntingford, C. and Jones, C.D. (2004)
- Amazonian forest dieback under climate-carbon cycle projections for the 21st Century. Theor.
- 792 *Appl. Climatol.* **78**, 137–156.
- 793 Craig, H. (1961) Isotopic variations in natural waters. *Science* **133**, 1702–1703.
- Dawson, T.E. (1998) Fog in the California redwood forest: ecosystem inputs and use by plants.
- 795 *Oecologia* 117, 476-485.
- Diefendorf, A.F., Freeman, K.H., Wing, S.L. and Graham, H.V. (2011) Production of n-alkyl
- 797 lipids in living plants and implications for the geologic past. *Geochim. Cosmochim. Acta* 75,
- 798 7472-7485.

- 799 Diefendorf, A.F., Leslie, A.B. and Wing, S.L. (2015) Leaf wax composition and carbon isotopes
- vary among major conifer groups. *Geochim. Cosmochim. Acta* **170**, 145-156.
- Dingemans, T., Mensing, S.A., Feakins, S.J., Kirby, M.E. and Zimmerman, S.H. (2014) 3000
- years of environmental change at Zaca Lake, California, USA. Front. Ecol. Evol. 2, doi:
- 803 10.3389/fevo.2014.00034.
- 804 Eller, C.B., Lima, A.L. and Oliveira, R.S. (2013) Foliar uptake of fog water and transport
- belowground alleviates drought effects in the cloud forest tree species, *Drimys brasiliensis*
- 806 (Winteraceae). New Phytol. 199, 151–162.
- 807 Ernst, N., Peterse, F., Breitenbach, S.F.M., Syiemlieh, H.J. and Eglinton, T.I. (2013) Biomarkers
- record environmental changes along an altitudinal transect in the wettest place on Earth. Org.
- 809 *Geochem.* **60**, 93–99.
- 810 Farquhar, G.D., Cernusak, L.A. and Barnes, B. (2007) Heavy water fractionation during
- 811 transpiration. *Plant Physiol.* **143**, 11–18.
- Feakins, S. and Sessions, A.L. (2010) Controls on the D/H ratios of plant leaf waxes from an arid
- ecosystem. Geochim. Cosmochim. Acta 74, 2128–2141.
- Feakins, S.J. (2013) Pollen-corrected leaf wax D/H reconstructions of northeast African
- hydrological changes during the late Miocene. *Palaeogeog. Palaeoclim. Palaeoecol.* **374**, 62–71.
- Feakins, S.J., Warny, S. and Lee, J.-E. (2012) Hydrologic cycling over Antarctica during the
- middle Miocene warming. *Nat. Geosci.* **5**, 557–560.
- 818 Galy, V., Eglinton, T., France-Lanord, C. and Sylva, S. (2011) The provenance of vegetation and
- environmental signatures encoded in vascular plant biomarkers carried by the Ganges-
- 820 Brahmaputra rivers. *Earth Planet. Sci. Lett.* **304**, 1–12.
- Gao, L., Edwards, E.J., Zeng, Y. and Huang, Y. (2014) Major Evolutionary Trends in Hydrogen
- Isotope Fractionation of Vascular Plant Leaf Waxes. *Plos One* **9**, e112610.

- Gao, L., Guimond, J., Thomas, E. and Huang, Y.S. (2015) Major trends in leaf wax abundance,
- delta H-2 and delta C-13 values along leaf venation in five species of C-3 plants: Physiological
- and geochemical implications. *Org. Geochem.* **78**, 144-152.
- 826 Garcin, Y., Schefuß, E., Schwab, V.F., Garreta, V., Gleixner, G., Vincens, A., Todou, G., Séné,
- O., Onana, J.-M., Achoundong, G. and Sachse, D. (2014) Reconstructing C3 and C4 vegetation
- cover using n-alkane carbon isotope ratios in recent lake sediments from Cameroon, Western
- 829 Central Africa. *Geochim. Cosmochim. Acta* **142**, 482–500.
- 630 Girardin, C.A.J., Espejob, J.E.S., Doughty, C.E., Huasco, W.H., Metcalfe, D.B., Durand-Baca,
- L., Marthews, T.R., Aragao, L., Farfan-Rios, W., Garcia-Cabrera, K., Halladay, K., Fisher, J.B.,
- 632 Galiano-Cabrera, D.F., Huaraca-Quispe, L.P., Alzamora-Taype, I., Eguiluz-Mora, L., Salinas-
- Revilla, N., Silman, M.R., Meir, P. and Malhi, Y. (2014a) Productivity and carbon allocation in a
- tropical montane cloud forest in the Peruvian Andes. *Plant Ecol. Divers.* 7, 107–123.
- Girardin, C.A.J., Farfan-Rios, W., Garcia, K., Feeley, K.J., Jorgensen, P.M., Murakami, A.A.,
- Perez, L.C., Seidel, R., Paniagua, N., Claros, A.F.F., Maldonado, C., Silman, M., Salinas, N.,
- Reynel, C., Neill, D.A., Serrano, M., Caballero, C.J., Cuadros, M.D.L., Macia, M.J., Killeen, T.J.
- and Malhi, Y. (2014b) Spatial patterns of above-ground structure, biomass and composition in a
- network of six Andean elevation transects. *Plant Ecol. Divers.* 7, 161–171.
- 640 Girardin, C.A.J., Malhi, Y., Aragao, L., Mamani, M., Huasco, W.H., Durand, L., Feeley, K.J.,
- Rapp, J., Silva-Espejo, J.E., Silman, M., Salinas, N. and Whittaker, R.J. (2010) Net primary
- productivity allocation and cycling of carbon along a tropical forest elevational transect in the
- 843 Peruvian Andes. *Glob. Chang. Biol.* **16**, 3176–3192.
- Goldsmith, G.R., Matzke, N.J. and Dawson, T.E. (2013) The incidence and implications of
- clouds for cloud forest plant water relations. *Ecol. Lett.* **16**, 307–314.
- 846 Gonfiantini, R., Roche, M., Olivery, J., Fontes, J. and Zuppi, G. (2001) The altitude effect on the
- isotopic composition of tropical rains. *Chem. Geol.* **181**, 147–167.

- Gotsch, S.G., Asbjornsen, H., Holwerda, F., Goldsmith, G.R., Weintraub, A.E. and Dawson, T.E.
- 849 (2014) Foggy days and dry nights determine crown-level water balance in a seasonal tropical
- montane cloud forest. *Plant, Cell Envir.* **37**, 261–272.
- Halladay, K., Malhi, Y. and New, M. (2012) Cloud frequency climatology at the Andes/Amazon
- transition: 1. Seasonal and diurnal cycles. J. Geophys. Res.: Atmos. 117, D23102.
- Horwath, A. (2011) *Epiphytic Bryophytes as Cloud Forest Indicators: Stable Isotopes, Biomass*
- and Diversity along an Altitudinal Gradient in Peru. University of Cambridge, pp. 284.
- Hou, J., D'Andrea, W. and Huang, Y. (2008) Can sedimentary leaf waxes record D/H ratios of
- continental precipitation? Field, model and experimental assessments. *Geochim. Cosmochimi.*
- 857 *Acta* **72**, 3503–3517.
- Hou, J.Z., D'Andrea, W.J., MacDonald, D. and Huang, Y. (2007) Hydrogen isotopic variability
- in leaf waxes among terrestrial and aquatic plants around Blood Pond, Massachusetts, USA. Org.
- 860 *Geochem.* **38**, 977–984.
- Hren, M.T., Pagani, M., Erwin, D.M. and Brandon, M. (2010) Biomarker reconstruction of the
- early Eocene paleotopography and paleoclimate of the northern Sierra Nevada. *Geology* **38**, 7–
- 863 10.
- Huacara Huasco, W., Girardin, C.A.J., Doughty, C.E., Metcalfe, D.B., Baca, L.D., Silva-Espejo,
- J.E., Cabrera, D.G., Aragao, L., Davila, A.R., Marthews, T.R., Huaraca-Quispe, L.P., Alzamora-
- Taype, I., Mora, L.E., Farfan-Rios, W., Cabrera, K.G., Halladay, K., Salinas-Revilla, N., Silman,
- 867 M.R., Meir, P. and Malhi, Y. (2014) Seasonal production, allocation and cycling of carbon in
- two mid-elevation tropical montane forest plots in the Peruvian Andes. *Plant Ecol. Divers.* 7,
- 869 125–142.
- Jia, G.D., Wei, K., Chen, F.J. and Peng, P.A. (2008) Soil n-alkane delta D vs. altitude gradients
- along Mount Gongga, China. Geochim. Cosmochim. Acta 72, 5165–5174.

- Kahmen, A., Hoffmann, B., Schefuß, E., Arndt, S.K., Cernusak, L.A., West, J.B. and Sachse, D.
- 873 (2013b) Leaf water deuterium enrichment shapes leaf wax n-alkane δD values of angiosperm
- plants II: Observational evidence and global implications. Geochim. Cosmochim. Acta 111, 50–
- 875 63.
- Kahmen, A., Schefuss, E. and Sachse, D. (2013a) Leaf water deuterium enrichment shapes leaf
- wax n-alkane delta D values of angiosperm plants I: Experimental evidence and mechanistic
- insights. Geochim. Cosmochim. Acta 111, 39–49.
- Kreft, H. and Jetz, W. (2007) Global patterns and determinants of vascular plant diversity. *Proc.*
- 880 Natl. Acad. Sci. U. S. A. 104, 5925–5930.
- Krull, E., Sachse, D., Mugler, I., Thiele, A. and Gleixner, G. (2006) Compound-specific d13C
- and d2H analyses of plant and soil organic matter: A preliminary assessment of the effects of
- vegetation change on ecosystem hydrology. Soil Biol. Biochem. 38, 3211–3221.
- Lavorel, S., Grigulis, K., McIntyre, S., Williams, N.S.G., Garden, D., Dorrough, J., Berman, S.,
- 885 Quétier, F., Thébault, A. and Bonis, A. (2008) Assessing functional diversity in the field –
- methodology matters! Funct. Ecol. 22, 134–147.
- Lee, J.E., Johnson, K. and Fung, I. (2009) Precipitation over South America during the Last
- 888 Glacial Maximum: An analysis of the "amount effect" with a water isotope-enabled general
- circulation model. *Geophys. Res. Lett.* **36**, L19701.
- 890 Li, S.G., Tsujimura, M., Sugimoto, A., Sasaki, L., Yamanaka, T., Davaa, G., Oyunbaatar, D. and
- Sugita, M. (2006) Seasonal variation in oxygen isotope composition of waters for a montane
- larch forest in Mongolia. *Trees* **20**, 122–130.
- Luo, P., Peng, P.A., Gleixner, G., Zheng, Z., Pang, Z.H. and Ding, Z.L. (2011) Empirical
- relationship between leaf wax n-alkane delta D and altitude in the Wuyi, Shennongjia and
- Tianshan Mountains, China: Implications for paleoaltimetry. Earth Planet. Sci. Lett. 301, 285–
- 896 296.

- Malhi, Y., Amezquita, F.F., Doughty, C.E., Silva-Espejo, J.E., Girardin, C.A.J., Metcalfe, D.B.,
- Aragao, L., Huaraca-Quispe, L.P., Alzamora-Taype, I., Eguiluz-Mora, L., Marthews, T.R.,
- Halladay, K., Quesada, C.A., Robertson, A.L., Fisher, J.B., Zaragoza-Castells, J., Rojas-Villagra,
- 900 C.M., Pelaez-Tapia, Y., Salinas, N., Meir, P. and Phillips, O.L. (2014a) The productivity,
- 901 metabolism and carbon cycle of two lowland tropical forest plots in south-western Amazonia,
- 902 Peru. *Plant Ecol. Divers.* **7**, 85–105.
- 903 Malhi, Y., Doughty, C.E., Goldsmith, G.R., Metcalfe, D.B., Girardin, C.A.J., Marthews, T.R.,
- del Aguila-Pasquel, J., Aragão, L.E.O.C., Araujo-Murakami, A., Brando, P., da Costa, A.C.L.,
- 905 Silva-Espejo, J.E., Farfán Amézquita, F., Galbraith, D.R., Quesada, C.A., Rocha, W., Salinas-
- 906 Revilla, N., Silvério, D., Meir, P. and Phillips, O.L. (2015) The linkages between photosynthesis,
- productivity, growth and biomass in lowland Amazonian forests. Glob. Chang. Biol. 21, 2283–
- 908 2295.
- 909 Malhi, Y., Gardner, T.A., Goldsmith, G.R., Silman, M.R. and Zelazowski, P. (2014b) Tropical
- 910 Forests in the Anthropocene. Ann. Rev. Envir. Res. 39, 125–159.
- 911 Malhi, Y., Silman, M., Salinas, N., Bush, M., Meir, P. and Saatchi, S. (2010) Introduction:
- 912 Elevation gradients in the tropics: laboratories for ecosystem ecology and global change
- 913 research. *Glob. Chang. Biol.* **16**, 3171–3175.
- Myers, N., Mittermeier, R.A., Mittermeier, C.G., da Fonseca, G.A.B. and Kent, J. (2000)
- 915 Biodiversity hotspots for conservation priorities. *Nature* **403**, 853–858.
- Newberry, S.L., Kahmen, A., Dennis, P. and Grant, A. (2015) n-Alkane biosynthetic hydrogen
- 917 isotope fractionation is not constant throughout the growing season in the riparian tree Salix
- 918 viminalis. *Geochim. Cosmochim. Acta* **165**, 75–85.
- Oyama, M.D. and Nobre, C.A. (2003) A new climate-vegetation equilibrium state for tropical
- 920 South America. Geophys. Res. Lett. 30.

- Paine, C.E.T., Baraloto, C. and Díaz, S. (2015) Optimal strategies for sampling functional traits
- 922 in species-rich forests. *Funct. Ecol.* 29, 1325–1331.
- Pearson, A. and Eglinton, T. (2000) The origin of n-alkanes in Santa Monica Basin surface
- sediment: a model based on compound-specific D14C and d13C data. Org. Geochem. 31, 1103–
- 925 1116.
- Peterse, F., van der Meer, M.T.J., Schouten, S., Jia, G., Ossebaar, J., Blokker, J. and Damste,
- J.S.S. (2009) Assessment of soil n-alkane delta D and branched tetraether membrane lipid
- distributions as tools for paleoelevation reconstruction. *Biogeosci.* **6**, 2799–2807.
- 929 Polissar, P.J. and Freeman, K.H. (2010) Effects of aridity and vegetation on plant-wax [delta]D
- in modern lake sediments. *Geochim. Cosmochim. Acta* **74**, 5785–5797.
- Polissar, P.J., Freeman, K.H., Rowley, D.B., McInerney, F.A. and Currie, B.S. (2009)
- Paleoaltimetry of the Tibetan Plateau from D/H ratios of lipid biomarkers. *Earth Planet. Sci.*
- 933 *Lett.* **287**, 64–76.
- Ponton, C., West, A.J., Feakins, S.J. and Galy, V. (2014) Leaf wax biomarkers in transit record
- 935 river catchment composition. *Geophys. Res. Lett.* **41**, 6420–6427.
- Porter, T.J., Froese, D.G., Feakins, S.J., Bindeman, I.N., Mahony, M.E., Pautler, B.G., Reichart,
- 937 G.-J., Sanborn, P.T., Simpson, M.J. and Weijers, J.W.H. (2016) Multiple water isotope proxy
- 938 reconstruction of extremely low last glacial temperatures in Eastern Beringia (Western Arctic).
- 939 Quat. Sci. Rev. 137, 113–125.
- Rapp, J.M. and Silman, M.R. (2012) Diurnal, seasonal, and altitudinal trends in microclimate
- across a tropical montane cloud forest. *Clim. Res.* **55**, 17–32.
- Sachse, D., Billault, I., Bowen, G.J., Chikaraishi, Y., Dawson, T.E., Feakins, S.J., Freeman,
- 943 K.H., Magill, C.R., McInerney, F.A., van der Meer, M.T.J., Polissar, P., Robins, R.J., Sachs, J.P.,
- 944 Schmidt, H.-L., Sessions, A.L., White, J.W.C., West, J.B. and Kahmen, A. (2012) Molecular

- Paleohydrology: Interpreting the Hydrogen-Isotopic Composition of Lipid Biomarkers from
- Photosynthesizing Organisms. Ann. Rev. Earth Planet. Sci. 40, 221–249.
- Sachse, D., Radke, J. and Gleixner, G. (2004) Hydrogen isotope ratios of recent lacustrine
- 948 sedimentary n-alkanes record modern climate variability. *Geochim. Cosmochim. Acta* 63, 4877–
- 949 4889.
- 950 Sachse, D., Radke, J. and Gleixner, G. (2006) dD values of individual n-alkanes from terrestrial
- 951 plants along a climatic gradient Implications for the sedimentary biomarker record. Org.
- 952 *Geochem.* **37**, 469–483.
- 953 Salati, E., Dallolio, A., Matsui, E. and Gat, J.R. (1979) Recycling of water in the Amazon Basin -
- 954 Isotopic study. *Water Resour. Res.* **15**, 1250–1258.
- Schefuss, E., Schouten, S. and Schneider, R. (2005) Climatic controls on central African
- 956 hydrology during the past 20,000 years. *Nature* **473**, 1003–1006.
- 957 Sessions, A.L. (2006) Seasonal changes in D/H fractionation accompanying lipid biosynthesis in
- 958 Spartina alterniflora. *Geochim. Cosmochim. Acta* 70, 2153–2162.
- 959 Sessions, A.L., Burgoyne, T.W., Schimmelmann, A. and Hayes, J.M. (1999) Fractionation of
- 960 hydrogen isotopes in lipid biosynthesis. *Org. Geochem.* **30**, 1193–1200.
- 961 Shanahan, T.M., Hughen, K.A., Ampel, L., Sauer, P.E. and Fornace, K. (2013) Environmental
- ontrols on the 2H/1H values of terrestrial leaf waxes in the eastern Canadian Arctic. *Geochim.*
- 963 *Cosmochim. Acta* **119**, 286–301.
- 964 Silman, M.R. (2014) Functional megadiversity. *Proc. Nat. Acad. Sci. U.S.A.* **111**, 5763–5764.
- Smith, F. and Freeman, K. (2006) Influence of physiology and climate on dD of leaf wax n-
- alkanes from C3 and C4 grasses. *Geochim. Cosmochim. Acta* **70**, 1172–1187.

- Ter Steege, H., (2010) Contribution of current and historical processes to patterns of tree
- diversity and composition of the Amazon, in: Hoorn, C., Wesselingh, F.P. (Eds.), Amazonia:
- *Landscape and Species Evolution.* Wiley (Oxford), 349–359.
- 970 Tierney, J.E., Smerdon, J.E., Anchukaitis, K.J. and Seager, R. (2013) Multidecadal variability in
- 971 East African hydroclimate controlled by the Indian Ocean. *Nature* **493**, 389–392.
- 972 Tipple, B.J., Berke, M.A., Doman, C.E., Khachaturyan, S. and Ehleringer, J.R. (2013) Leaf-wax
- 973 *n*-alkanes record the plant–water environment at leaf flush. *Proc. Nat. Acad. Sci. U.S.A.* **110**,
- 974 2659–2664.
- 975 Tipple, B.J. and Pagani, M. (2013) Environmental control on eastern broadleaf forest species'
- 976 leaf wax distributions and D/H ratios. Geochim. Cosmochim. Acta 111, 64–77.
- Viviroli, D., Dürr, H.H., Messerli, B., Meybeck, M. and Weingartner, R. (2007) Mountains of
- 978 the world, water towers for humanity: Typology, mapping, and global significance. *Water*
- 979 Resour. Res. 43, W07447.
- 980 West, J.B., Sobek, A. and Ehleringer, J.R. (2008) A Simplified GIS Approach to Modeling
- 981 Global Leaf Water Isoscapes. *PLoS ONE* 3, e2447.
- Wilkie, K.M.K., Chapligin, B., Meyer, H., Burns, S., Petsch, S. and Brigham-Grette, J. (2013)
- 983 Modern isotope hydrology and controls on δD of plant leaf waxes at Lake El'gygytgyn, NE
- 984 Russia. Clim. Past 9, 335–352.
- 985 Winnick, M.J., Chamberlain, C.P., Caves, J.K. and Welker, J.M. (2014) Quantifying the isotopic
- 'continental effect'. Earth Planet. Sci. Lett. 406, 123–133.
- 287 Zelazowski, P., Malhi, Y., Huntingford, C., Sitch, S. and Fisher, J.B. (2011) Changes in the
- 988 potential distribution of humid tropical forests on a warmer planet. Phil. Trans. Royal Soc. A
- 989 **369**, 137–160.

Zhou, Y.P., Grice, K., Stuart-Williams, H., Farquhar, G.D., Hocart, C.H., Lu, H. and Liu, W.G.
(2010) Biosynthetic origin of the saw-toothed profile in delta(13) C and delta H-2 of n-alkanes
and systematic isotopic differences between n-, iso- and anteiso-alkanes in leaf waxes of land
plants. *Phytochem.* 71, 388–403.

**Table 1.** Environmental and ecological characteristics of 1-ha study plots along a tropical montane elevation gradient.

CHAMBASA plot code	Tambopata 6	Tambopata 5	San Pedro 2	San Pedro 1	Esperanza
RAINFOR site code	TAM-06	TAM-05	SPD-02	SPD-01	ESP-01
Latitude	-12.8385	-12.8309	-13.0491	-13.0475	-13.1751
Longitude	-69.2960	-69.2705	-71.5365	-71.5423	-71.5948
Elevation* (m)	215	223	1494	1713	2868
Slope* (deg)	2.2	4.5	27.1	30.5	27.3
Aspect* (deg)	169	186	125	117	302
Solar radiation (GJ m <sup>-2</sup> a <sup>-1</sup> )	4.8	4.8	4.08	4.36	n/a
Mean annual air					
temperature** (°C)	24.4	24.4	18.8	17.4	13.1
Precipitation (mm a <sup>-1</sup> )	1900	1900	5302	5302	1560
Soil moisture (%)	35.5	21.8	37.3	37.6	24.3
Vegetation height*	28.2	27.5	22.8	14.0	16.9

\*Derived from high-resolution airborne Light Detection and Ranging (LiDAR) data (see Asner et al. 2013 for methodology). \*\*Derived from observations between 6 Feb 2013 and 7 Jan 2014.

## Figure Legends

1001

1028

1002 Fig. 1: Illustration of sample locations. See Appendix A for interactive map of sample location. Fig. 2: Dual oxygen and hydrogen isotopic analysis of environmental and plant waters. (a) 1003 1004 Meteoric waters including cloud water (grey circles), instantaneous precipitation samples (light blue circles; both Clark et al., 2014), biweekly integrations of precipitation (dark blue circles, 1005 1006 LMWL) and stream waters differentiating wet and dry season (open and solid black squares respectively; both Ponton et al., 2014 and this study), with regressions. (b) Plant xylem (XW; 1007 1008 orange diamonds) and leaf waters (LW; green triangles) both collected during the dry season, 1009 showing cloud and LMWL regressions from A for comparison. Inset: schematic of water sources 1010 and processes. Fig. 3: Elevation gradients in plant xylem water (diamonds), leaf water (triangles) and leaf wax 1011 1012 hydrogen isotopic composition (circles) (a) for the  $C_{28}$  *n*-alkanoic acids and (b) for the  $C_{29}$  *n*alkanes. Data shown are for individual samples, which include mixed species with replicate 1013 1014 sampling of each species (small symbols), regression line and statistics (for LW and XW see a). Also shown, site averages for each variable (large symbols). Note two sites TAM-05 and TAM-1015 06 are both very close to 0.2 km asl and therefore the two sites overlay at this elevation scale. 1016 1017 **Fig. 4**: Relationships between plant water  $\delta D$  and plant leaf wax  $\delta D$  values: (a) Xylem water vs. 1018 *n*-alkanoic acids, (b) leaf water vs. *n*-alkanoic acids, (c) xylem water vs. *n*-alkanes, and (d) leaf water vs. *n*-alkanes. Showing data for all homologues, regression lines only where relationships 1019 are significant. Xylem water is significantly correlated with leaf wax isotopic composition for all 1020 homologues with widespread presence; note that the longer chain n-alkanoic acids ( $C_{30}$  and  $C_{32}$ ) 1021 1022 are not found at the higher elevation sites (more negative  $\delta D_{XW}$  values). Leaf water is generally not significantly correlated with leaf wax isotopic composition (see text). 1023 1024 Fig. 5: Conceptual diagram showing tropical forest hydrogen isotope systematics, summarizing isotope-relevant fluxes (lines) fractionations (arrows) and compositions (boxes). The apparent 1025 fractionation  $\varepsilon_{app}$  (dotted arrow) is a net effect and key to geological applications of the proxy, 1026 1027 determined here directly as  $\varepsilon_{\text{wax/XW}}$  and  $\varepsilon_{\text{wax/w}}$ . Precipitation varies between storms and seasons

but its time-averaged composition is reflected in xylem water. Leaf water may be enriched via

1029 transpiration but equilibration with atmospheric vapor at high relative humidity (RH) and foliar 1030 uptake in the TMCF means the enrichment of leaf water over xylem water ( $\varepsilon_{XW/LW}$ ; dashed line) is minimal. Biosynthetic fractionation ( $\varepsilon_{bio}$ ) is the fractionation between substrate (water) and the 1031 1032 product (wax) that occurs within the leaf and estimated by bulk leaf water measured at a single 1033 point in time (dry season, early afternoon) in this study ( $\varepsilon_{\text{wax/LW}}$ ). Modified after Sachse et al. 1034 (2006). Y-dimension denotes hydrogen isotopic composition. X-dimension denotes fluxes. Scaling and shading for illustrative purposes only. Inset: photo of tropical forest with cloud at 1035 foothills of the Andes taken at ca. 500 m asl. 1036 1037 **Fig. 6**: Apparent fractionations ( $\varepsilon_{\text{wax/w}}$ ) across the elevation transect, weighting for individual species contributions. a) Bubble plot weighing individual data for wax loading for C<sub>29</sub> n-alkane 1038 and (b) for C<sub>28</sub> n-alkanoic acid. (c) Summary plot showing mean unweighted values for all 1039 1040 individuals, as well as weighted means that account for wax concentration of species and 1041 community-weighted means that account for both wax concentration and proportional species 1042 representation in each forest plot for C<sub>29</sub> n-alkane, and (d) for C<sub>28</sub> n-alkanoic acid. Overall unweighted mean apparent fractionation (black solid line, and  $\pm 1 \sigma$  dotted lines) shown. (e) 1043 1044 Community representation: fraction of basal area represented by sampling (pie charts), with 1045 number of individuals and species sampled. Fig. 7: Elevation trends in  $\delta D$  values weighted for individual species contributions. (a) Bubble 1046 plot weighing individual data for wax loading for  $C_{28}$  *n*-alkanoic acid and (b) for  $C_{29}$  *n*-alkane. 1047 (c) Summary plot showing mean unweighted values for all individuals, as well weighted means 1048 1049 that account for wax concentration of species and community-weighted means that account for both wax concentration and proportional species representation in the forest plot for C<sub>29</sub> n-1050 1051 alkane, and (d) for C<sub>28</sub> *n*-alkanoic acid. The unweighted and weighted means are not significantly 1052 different. Error bars  $(1\sigma)$  and regression shown for the community-weighted means only. Regression is sensitive to the exclusion (solid line) or inclusion of SPD-01 outlier (open symbol, 1053 1054 dashed line) as shown in (c). 1055 Fig. 8: Tropical forest calibration using community-weighted plot mean  $\delta D$  values relative to

source water  $\delta D$  values for both the  $C_{29}$  *n*-alkane (red) and the  $C_{28}$  *n*-alkanoic acid (gold),

1056

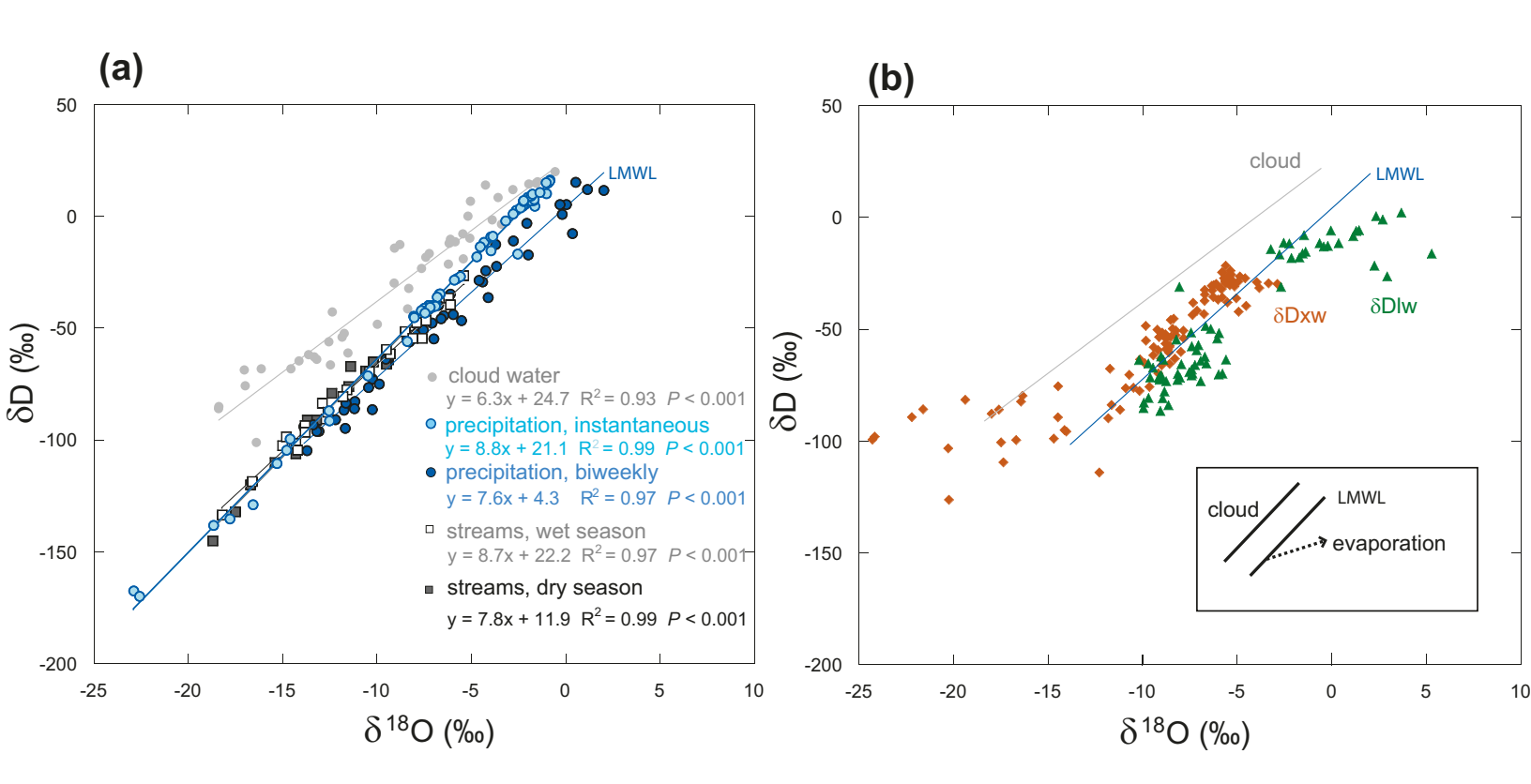
excluding one outlier (SPD-01  $C_{28}$  *n*-alkanoic acid) as in Fig. 7. Ordinary least squares regression (solid line), 95% confidence intervals (dashed line), extrapolation (dotted line) to intercept ( $\varepsilon_{\text{wax/w}}$ ). Relationship of slope and intercept is in the form  $y = \alpha x + \varepsilon$ , and within uncertainties meets expectations that  $\alpha = 1 - \varepsilon$  (from Eq. 1) as well as being similar to  $\varepsilon_{\text{wax/w}}$  or  $\varepsilon_{\text{wax/XW}}$  calculated as the average of individuals (Appendix A).

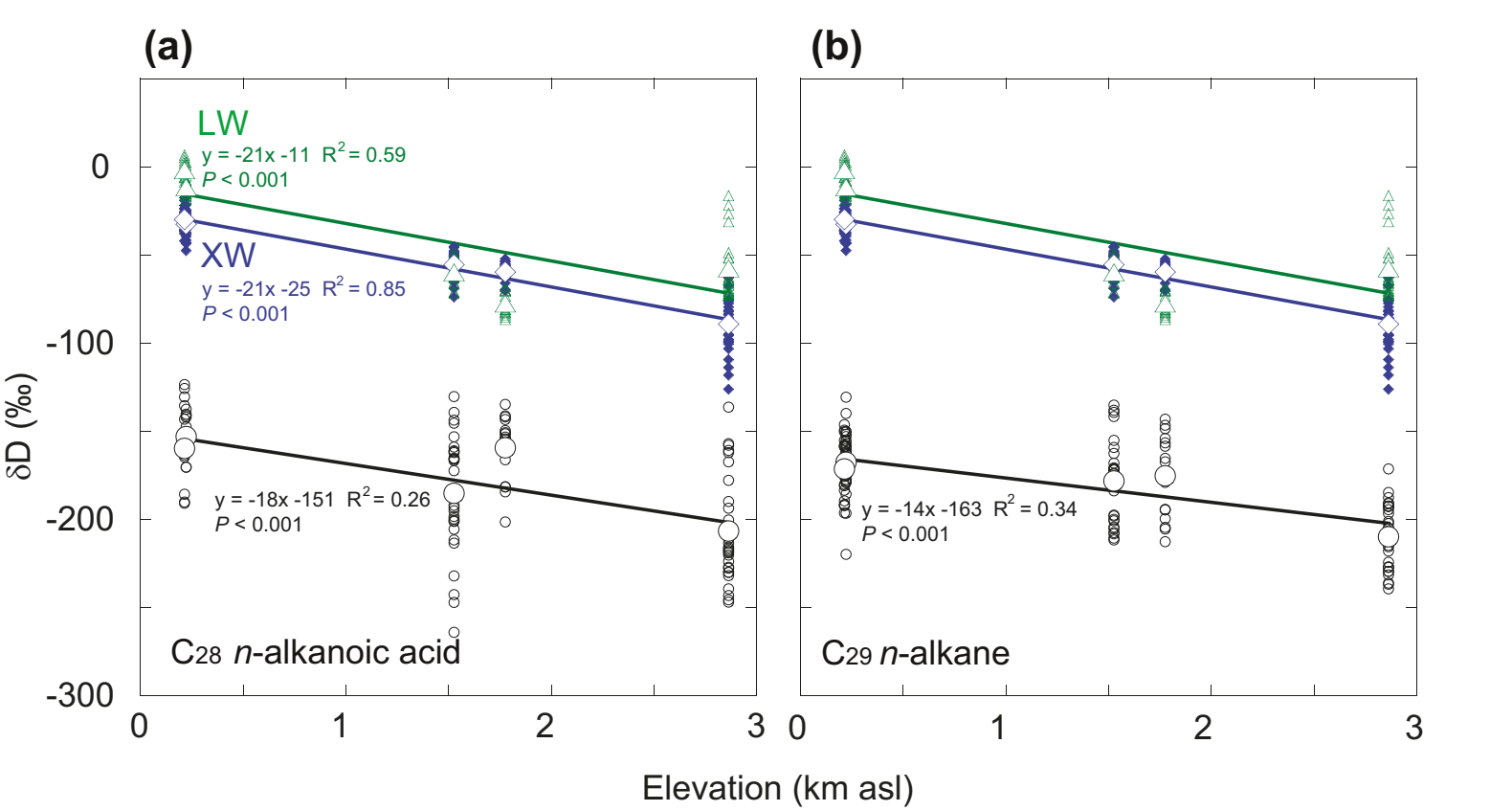
Tropical
Montane
Cloud Forest

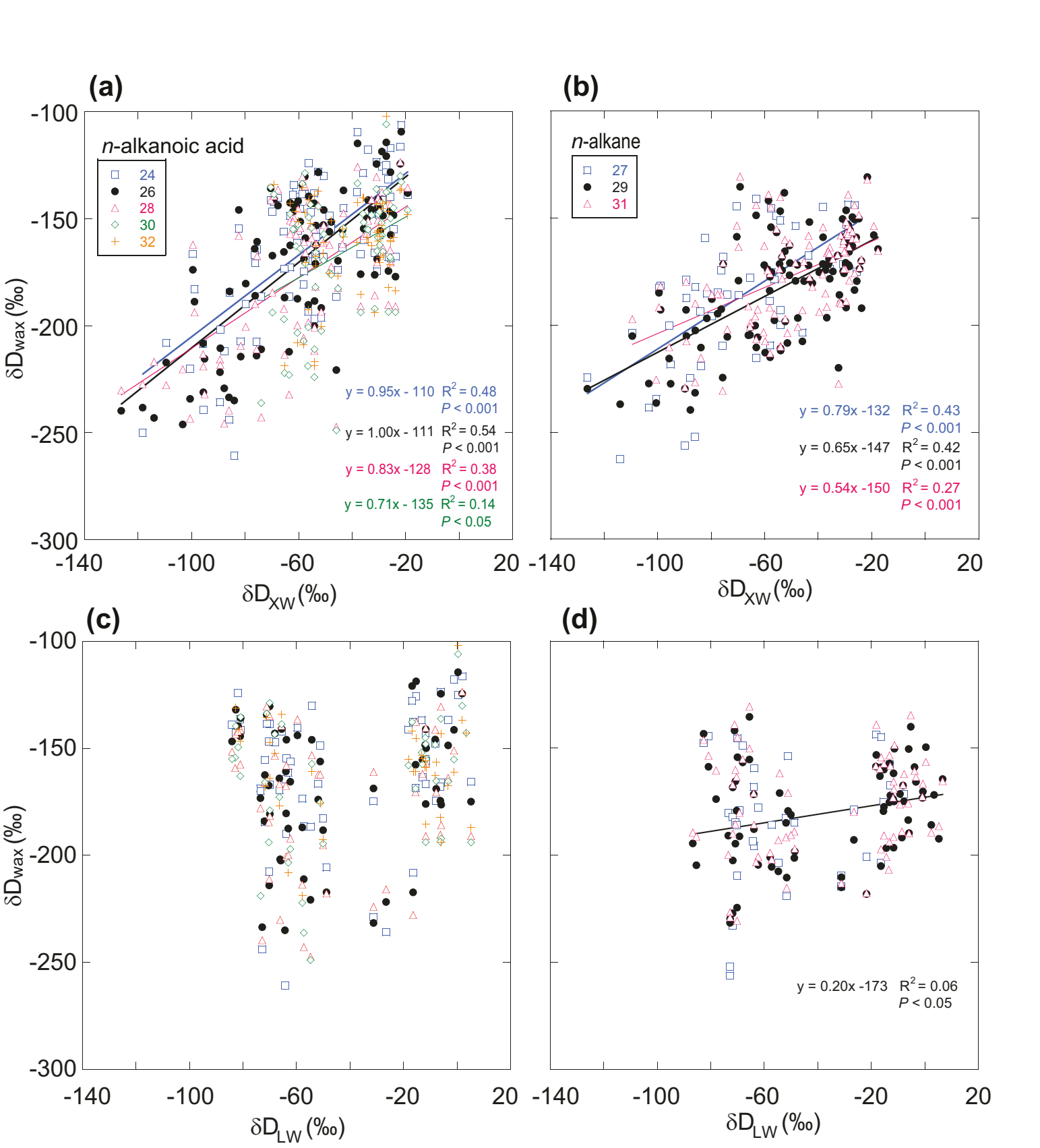
Tropical SPD-01, 1.7km asl, above cloud base

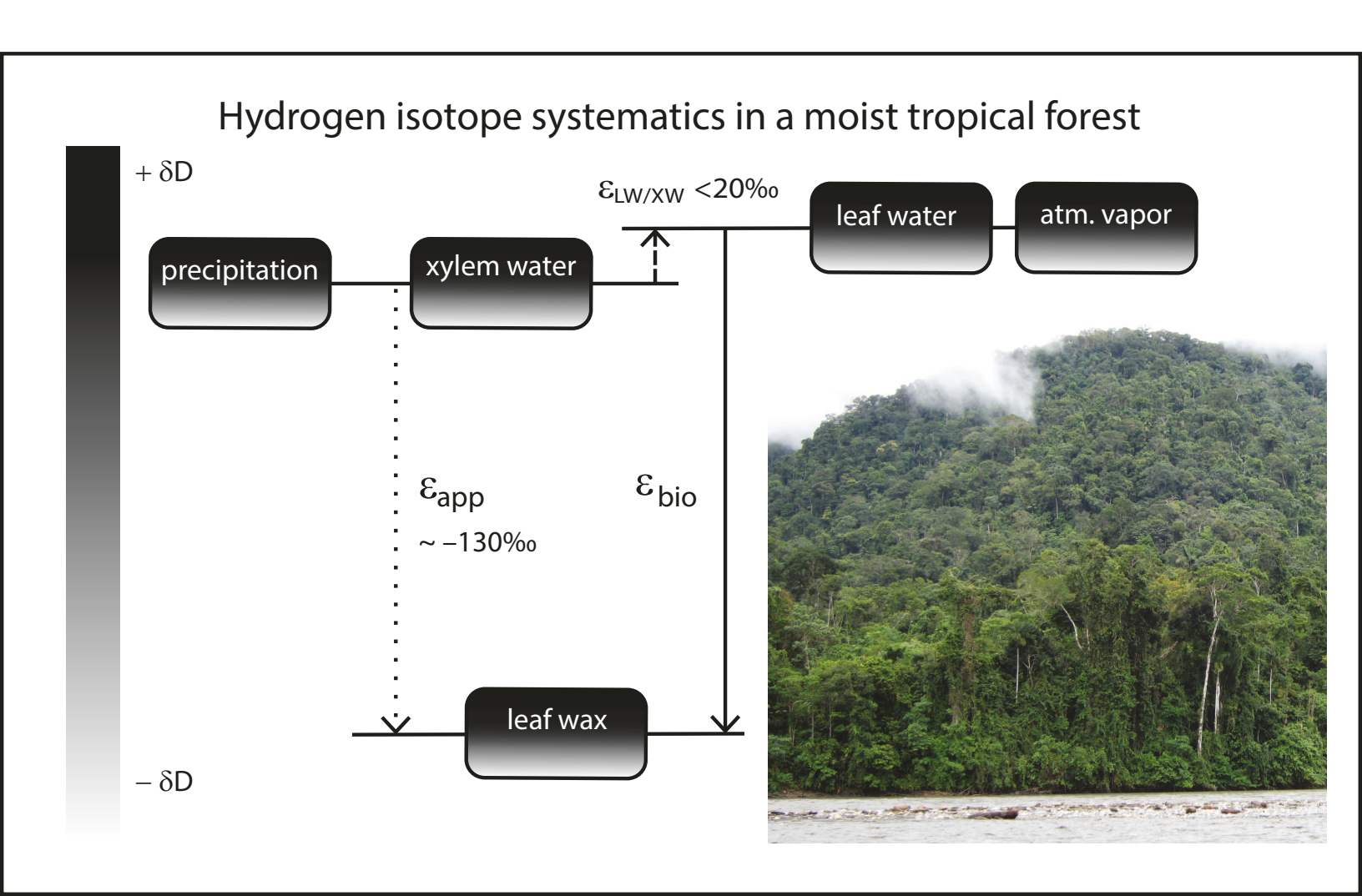
SPD-02, 1.5km asl, below cloud base

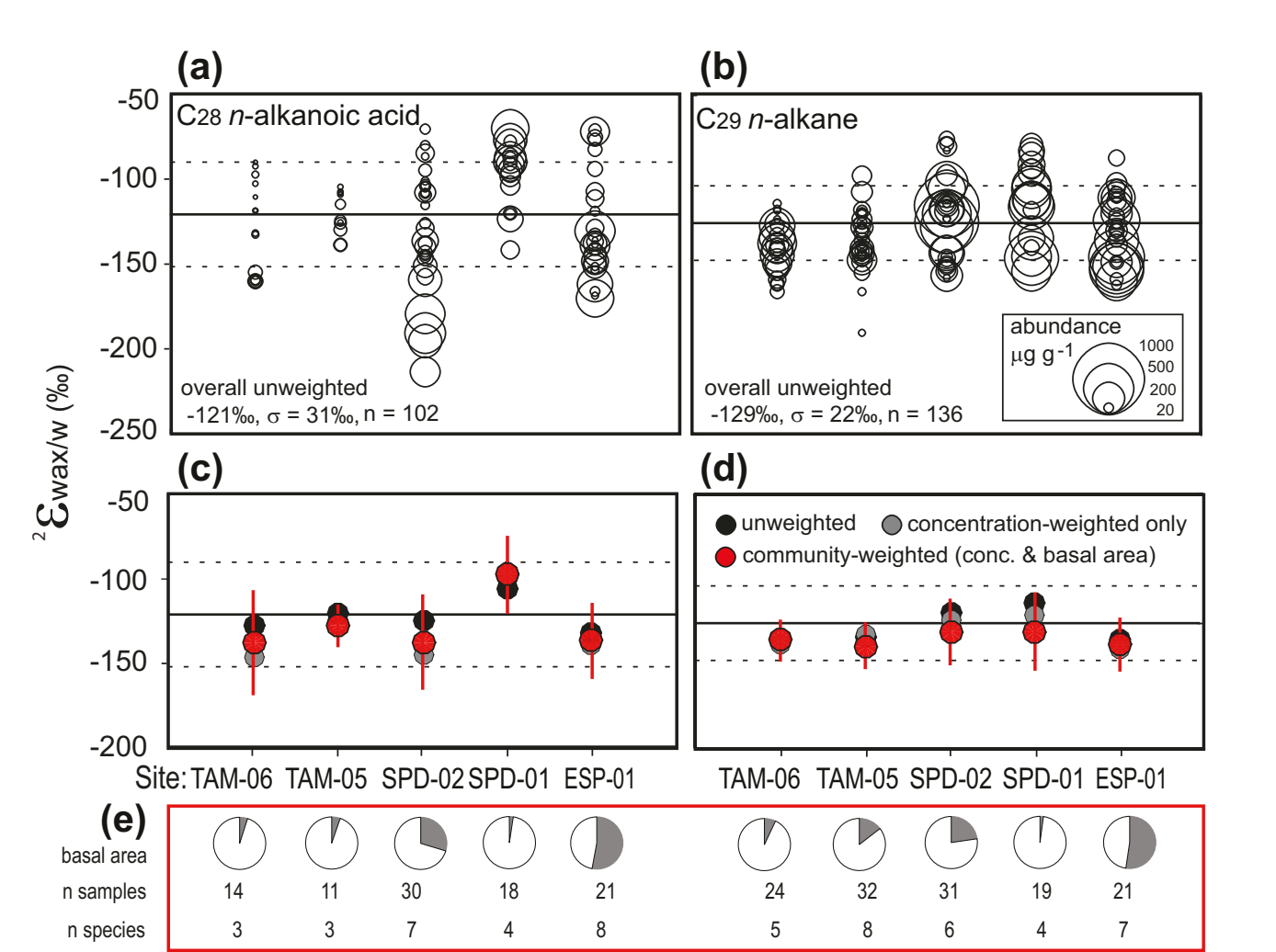
0.2km asl
TAM-05 TAM-06
river-distal river-proximal

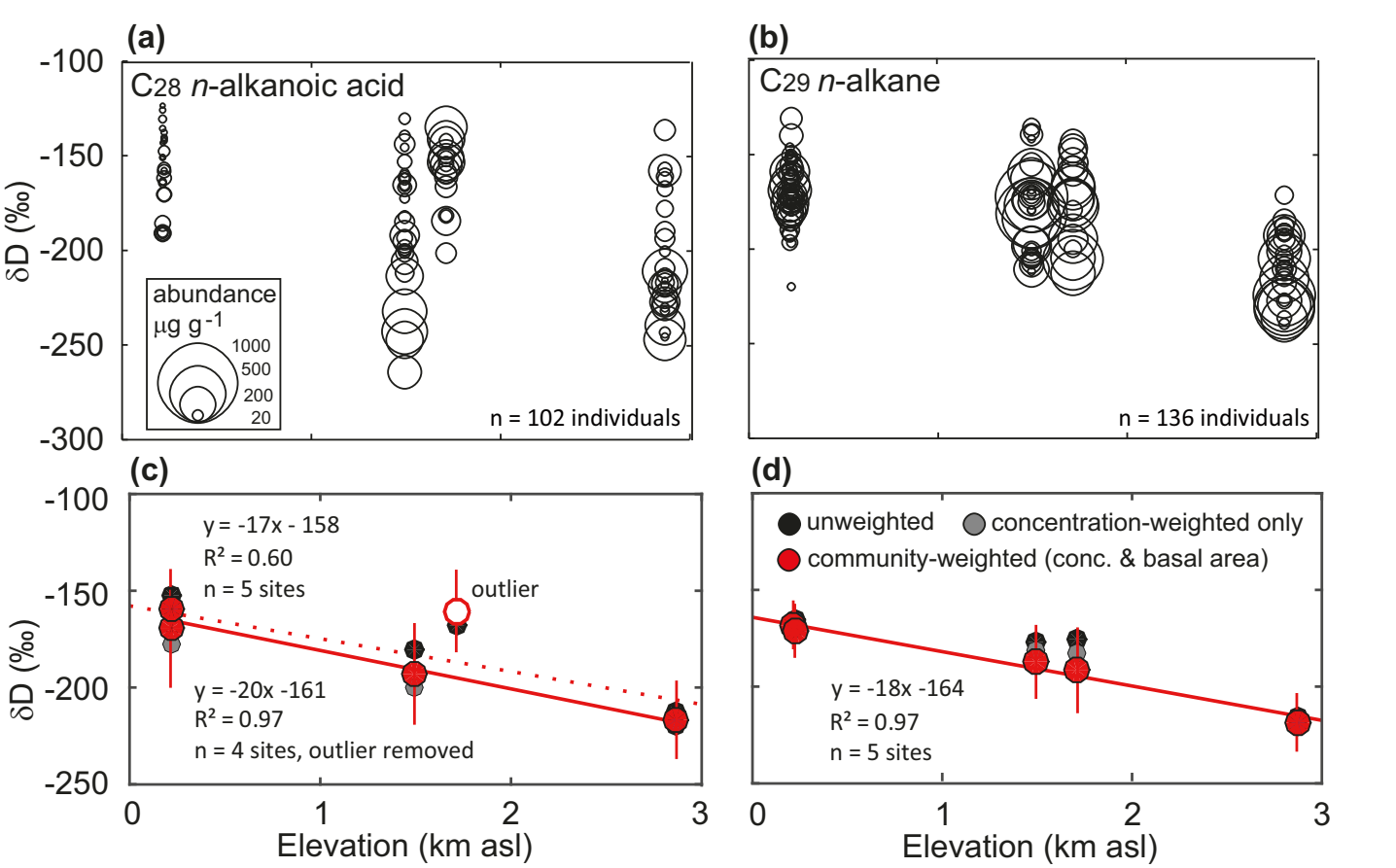


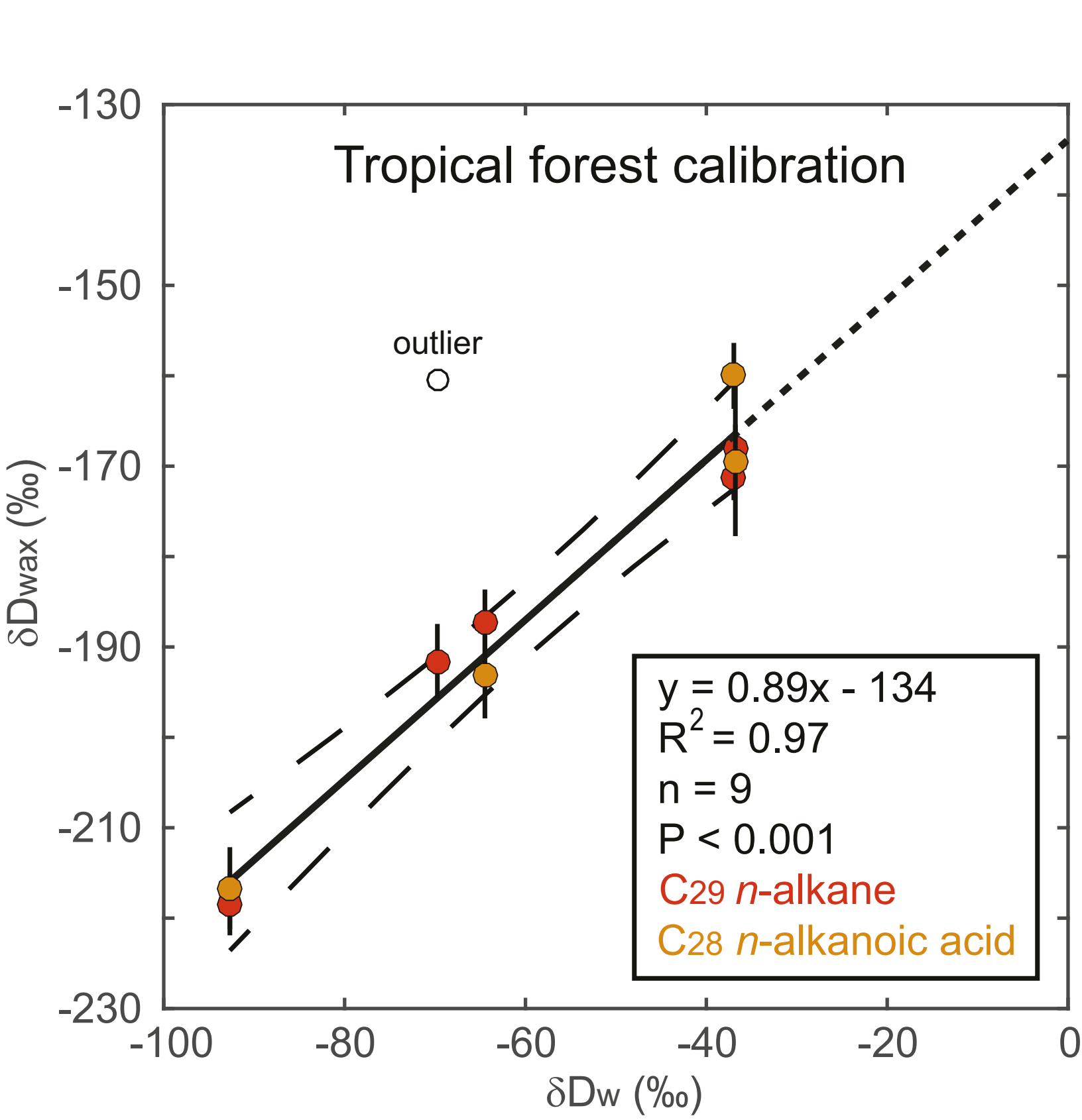












Appendix Click here to download Appendix: Appendix A.xlsx

Interactive Map file (.kml or .kmz)
Click here to download Interactive Map file (.kml or .kmz): PeruPlantSites.kml